Structural circuit plasticity by a neurotrophin with a Toll modifies dopamine-dependent behaviour

Jun Sun[1], Suzana Ulian-Benitez[1,2], Manuel G. Forero[3], Guiyi Li[1], Deepanshu Singh[1], Sebastian Cachero[4], Francisca Rojo-Cortés[1], Marta Moreira[1], Dean Kavanagh[5], Gregory Jefferis[4] and Alicia Hidalgo[1*]

1, Structural Plasticity & Regeneration Group, School of Biosciences, University of Birmingham, UK;

2, current address: Buck Institute for Research on Aging, California, US;

3, Universidad Señor de Sipán, Chiclayo, Perú;

4, MRC LMB, Cambridge, UK;

5, Institute of Biomedical Research, University of Birmingham, UK.

*Author for correspondence:

00 44 (0)121 4145416

a.hidalgo@bham.ac.uk

Short running title: Novel molecular mechanism of circuit plasticity

Keywords: structural brain plasticity, neurodegeneration, neuronal activity, dopamine, neurotrophin, *Drosophila* neurotrophin 2, DNT-2, Toll, Toll-Like Receptor, Kekkon, Kek, TrkB, TrkB-T1, TrkC-T1

ABSTRACT

Toll receptors are expressed in the distinct anatomical brain modules and can regulate structural brain plasticity in adult *Drosophila*. Structural plasticity in response to neuronal activity and experience could enable adaptation, and its deficit could underlie brain dysfunction and disease. Thus, a key goal is to understand how structural circuit changes modify behaviour. Subjective experience requires dopamine, a neuromodulator that controls arousal, motivation and locomotion, and assigns a value to stimuli. *Toll-6* is expressed in dopaminergic neurons (DANs), raising the intriguing possibility that Toll-6 could regulate plasticity in dopaminergic circuits. Drosophila neurotrophin-2 (DNT-2) is the ligand for Toll-6, but it is unknown whether it is required for structural circuit plasticity. Here, we show that structural plasticity depends on the activity-dependent increase and activation of DNT-2, which in turn functions via its Toll-6 and kinase-less Trk-like Kek-6 receptors in DANs, modifying behaviour. *DNT-2* expressing neurons are anatomically and functionally connected with DANs, and they modulate each other. Loss of *DNT-2* or *Toll-6* and *kek-6* function caused DAN loss and synapse loss, and alterations in their levels compromised dendritic size and complexity and axonal targeting of analysed single neurons. Neuronal activity-dependent synapse formation required DNT-2, Toll-6 and Kek-6. Furthermore, structural plasticity in an associative, dopaminergic circuit modified dopamine-dependent behaviours, including locomotion and long-term memory. We conclude that an activity-dependent feedback loop involving dopamine and DNT-2 labelled the circuits engaged, and DNT-2 with Toll-6 and Kek-6 induced structural plasticity in this circuit, modifying behaviour.

INTRODUCTION

How experience shapes neural circuits and how this in turn modifies brain function and behaviour, is poorly understood. Toll receptors are expressed in distinct and overlapping patterns marking the anatomical brain domains in adult *Drosophila*, and as they can drive diverse signalling outcomes, they are ideally placed to translate experience into structural brain change [1]. Toll-2 promotes adult neurogenesis and it maintains neuronal survival, and loss of *Toll-2* function causes neurodegeneration – loss of neurons, axons and

dendrites - and it impairs locomotion [1]. Furthermore, neuronal-activity increases cell number in the adult brain in a Toll-2 dependent manner [1]. At least seven *Tolls* are expressed in the adult brain, and they could potentially cause distinct cellular outcomes depending on which Tolls and adaptors are activated in different cellular contexts [1, 2]. In nervous system development, signalling by Toll receptors can promote either cell survival or cell death, cell quiescence or cell proliferation, axon targeting and synaptogenesis [1-3]. In the mammalian brain, neuronal activity can also influence neurogenesis and gliogenesis, cell survival and death, growth and retraction of dendritic and axonal arborisations, formation and elimination of synapses, modifying circuit connectivity [4-8]. Structural plasticity is the formation of new neurons, neurites or synapses as a result of neuronal activity. In principle, structural plasticity could enable the brain to adapt to environmental stimuli and experience, but it is not necessarily adaptive, and instead can reflect opportunistic connections between neurons that do not benefit behaviour [7]. On the other hand, structural homeostasis is the decrease in dendritic arbours, elimination of neurites and synapses, which constrains change within boundaries that enable appropriate behaviour, but it can drive degenerative processes, such as in ageing, stress, and brain disease (e.g. neurodegenerative and psychiatric) [4, 5, 9]. The balance between structural plasticity and homeostasis underlies normal behaviour, whereas loss of structural plasticity accompanies brain disease [10]. In fact, anti-depressants work by inducing structural and functional plasticity [11, 12]. Thus, a key goal is to understand whether and how activity-dependent structural brain change modifies behaviour. Here, we ask whether Tolls could provide a molecular link between structural circuit plasticity and behaviour.

The *Drosophila* adult brain is plastic and can also be modified by experience and neuronal activity [13-21]. Different living conditions such as light vs. darkness, isolation vs. crowding, single vs. mixed sexes, modify brain volume and fibre number [13-15, 22]. Neuronal activation is commonly used as proxy of experience to investigate structural plasticity [18]. Stimulation with odorants or light, neuronal activation or silencing, circadian rhythms and long-term memory, modify glomerular volume, alter circuit and neuronal shape, and remodel synapses, revealing both experience-dependent structural plasticity and homeostasis [16-18, 21, 23-28]. Furthermore, the *Drosophila* brain is also susceptible to neurodegeneration [29].

However, molecular mechanisms underlying structural brain plasticity and homeostasis are limited in mammals and unknown in *Drosophila*. Toll receptors could be involved, but how they might link structural circuit remodelling to the modulation of behaviour remains unexplored.

We had previously observed that in the adult brain, *Toll-6* is expressed in dopaminergic neurons [3]. Dopamine is a neuromodulator required for both experience and behaviour, raising the intriguing possibility that Toll-6 might regulate structural plasticity in dopaminergic circuits, in turn modifying behaviour. Dopamine is a key neuromodulator that regulates wakefulness and motivation, experience valence, such as reward, and it is essential for locomotion, learning and memory [30-34]. Dopaminergic neurons (DANs) form an associative neural circuit together with mushroom body Kenyon cells (KCs), Dorsal Anterior Lateral neurons (DAL) and Mushroom Body Output neurons (MBONs) [32, 35, 36]. Kenyon cells receive input from projection neurons of the sensory systems, they then project through the mushroom body lobes where they are intersected by DANs to regulate MBONs to drive behaviour [32, 35]. DAL neurons are required for long-term memory [36]. This associative circuit involving KCs, DANs, DAL and MBONs is required for learning, long-term memory and goal-oriented behaviour [33, 36-39]. During experience, involving sensory stimulation from the external world and from actions, dopamine assigns a value to otherwise neutral stimuli, labelling the associative neural circuits engaged. Thus, a link to dopamine could enable Toll-6 to translate experience into circuit modification and modulate behaviour.

Toll receptors function in nervous system development and brain plasticity, cell rearrangements and cell competition, and Toll-1 also has functions in innate immunity [1-3, 40-44]. Some of these functions require nuclear downstream signalling, which is normally activated by ligand binding. In the central nervous system (CNS), Tolls can promote cell survival and cell quiescence via MyD88, ERK and NFκB/Dorsal downstream; cell proliferation via Wek and Yki; cell death via Wek, Sarm and JNK; and microtubule dynamics via Sarm, FoxO and Pavarotti [1-3, 45]. Tolls can also function independently of ligand binding and of nuclear signalling, via cell-cell interactions, such as for circuit connectivity and cell rearrangements, and outside the CNS, in planar cell polarity, where they link to Src and PI3K [42-44]. Toll receptors in Drosophila are bound by Spätzle (Spz) protein family ligands, also known as *Drosophila* neurotrophins (DNTs), that are

sequence, structural and functional homologues of the mammalian neurotrophins [2, 3, 46-51]. During embryonic development, Toll-6 and Toll-7 function as neurotrophin receptors for DNT-2 and DNT-1, respectively, to promote cell survival and connectivity [3]. Importantly, the targets regulated by Tolls - ERK, NFκB, PI3K, JNK – are also regulated by neurotrophin signalling in mammals and have key roles in structural and functional plasticity across the animals [2, 43, 52, 53]. However, whether Tolls regulate circuit plasticity and whether this might depend on their ligands, is unknown.

The Toll orthologues in vertebrates are the Toll-Like Receptors (TLRs), and Tolls and TLRs across the animals have universal functions in innate immunity [54]. However, mammalian TLRs are pattern recognition receptors (PRR) that directly bind pathogens and damage associated molecular patterns (PAMPs and DAMPs), whereas *Drosophila* Tolls are not, and they bind Spz family ligands instead [54, 55]. Remarkably, mammalian *TLRs* are expressed in all CNS cell types, where they can regulate neurogenesis, apoptosis, neurite growth and retraction, and synaptogenesis – independently of immunity [56-61]. However, their functions in structural brain plasticity and behaviour remain little explored.

DNTs are also ligands for Kekkons (Kek), Trk-like receptors in *Drosophil*a lacking a kinase domain [62, 63]. Mammalian Trks are receptors for neurotrophins (NTs, comprising: NGF, BDNF, NT3, NT4), and they function primarily via tyrosine kinase signalling [64]. In mammals, NTs bind Trk receptors to promote cell survival, connectivity, synaptogenesis, synaptic potentiation, learning and long-term memory, and they can also bind $p75^{NTR}$ receptors to promote cell survival or cell death, growth cone collapse, synapse loss and long-term depression [11, 52, 65, 66]. Kinase-less Trk isoforms are abundant in the mammalian adult brain and are linked to psychiatric disorders, but their functions remain poorly understood [67]. The *Drosophila* genome lacks full-length Trk receptors, but *keks* are *Trk* homologues lacking the kinase domain [62, 63]. There are six *kek* paralogous genes, at least four are expressed in the nervous system and some Keks can bind DNTs promiscuously [63, 68]. DNT-2 secreted from the muscle binds Kek-6 in motoneurons, which activates CaMKII pre-synaptically to regulate axonal terminal growth and structural synaptic plasticity [63]. CaMKII is highly evolutionarily conserved and has a critical role in structural and functional synaptic plasticity, learning and long-term memory [69]. At the NMJ, DNT-2 binds a receptor complex formed of

Toll-6 and Kek-6 [63]. Thus, DNT-2 is a ligand for Toll-6 and Kek-6, although it could also bind other Tolls and Keks promiscuously [3, 63]. NTs are involved in structural brain plasticity in mammals, but the extreme complexity of their pleiotropic functions and circuits involved has challenged progress [10, 11, 52, 65, 70]. Whether *Drosophila* neurotrophins regulate structural brain plasticity has not previously been investigated. And whether NTs, TLRs and kinase-less Trks are functionally related in the mammalian brain has not been explored either.

Here, we asked whether the neurotrophin ligand DNT-2 functions with its receptors Toll-6 and Kek-6 to regulate structural plasticity in the adult *Drosophila* brain. As Toll-6 is expressed in dopaminergic neurons, we analysed dopamine-dependent behaviours as readout of circuit modification. The findings revealed that neuronal activity caused dopamine to label neural circuits engaged, and these were then sculpted by a growth factor functioning via a Toll, resulting in the modification of behaviour.

RESULTS

DNT-2A, Toll-6 and Kek-6 neurons are integrated in a dopaminergic and associative circuit

To allow detailed anatomical and functional analyses of *DNT-2* expressing neurons, we generated a *DNT-2Gal4* line using CRISPR/Cas9. We used *DNT-2Gal4* to drive expression of the membrane-tethered-GFP *FlyBow1.1* reporter and identified at least 12 DNT-2+ neurons (Figure S1A). We focused on four anterior DNT-2A neurons per hemi-brain (Figure 1A). Using the post-synaptic marker Denmark, we identified DNT-2A dendrites at the prow (PRW) and flange (FLA) region, whereas axonal terminals visualised with the pre-synaptic marker synapse defective 1 (Dsyd1-GFP) resided at the superior medial protocerebrum (SMP) (Figure 1B,D). We additionally found post-synaptic signal at the SMP and pre-synaptic signal at the FLA/PRW (Figure 1D), indicative of bidirectional communication at both sites. To visualize individual DNT-2A cells, we generated single neuron Multi-Colour Flip-Out (MCFO) clones [71, 72] (Figure 1C). This approach revealed variability in the DNT-2A projections across individual flies (Figure 1A,C), consistently with developmental and activity-dependent structural plasticity in Drosophila [1, 15-19, 73]. We found that DNT-2A neurons are glutamatergic as they express the vesicular glutamate transporter vGlut (Figure 1E)

and lack markers for other neurotransmitter types (Figure S1B,E,F,G,H,I,J). DNT-2A terminals overlapped with those of octopaminergic (Figure S1E) and dopaminergic neurons (Figure 1F), suggesting they could receive inputs from neuromodulatory neurons. At the SMP, DNT-2A axonal terminals closely apposed arborisations from PPL1 and PAMs dopaminergic neurons (Figure 1F, right). Single-cell RNA-seq data revealed that DNT-2+ neurons can express the dopamine receptors *DopR1, Dop2R* or *DopEcR* [74]. Using reporters, we found that DopR2 is present in DNT-2A neurons, but not DopR1 (Figure 1E right, Figure S1D). Altogether, these data showed that DNT-2A neurons are excitatory glutamatergic neurons that could receive dopaminergic input both at PRW and SMP.

DNT-2 functions via Toll-6 and Kek-6 receptors, although it can bind various Tolls and Keks promiscuously [2, 3], and *Toll-6* is expressed in DANs [3]. To identify the cells expressing *Toll-6* and *kek-6* and explore further their link to the dopaminergic system, we used *Toll-6Gal4* and *kek-6Gal4* to drive expression of membrane-tethered *FlyBbow1.1* and assessed their expression throughout the brain. Using anti-Tyrosine Hydroxilase (TH) - the enzyme that catalyses the last step in dopamine synthesis - to visualise DANs, we found that Toll-6+ neurons included 30% PAMs, as well as PPL1 and PPL2 (Figure 1H, Figure S2D,G Table S1), whilst Kek-6+ neurons included PAM, PAL, PPL1, PPM2 and PPM3 dopaminergic clusters (Figure 1I, Figure S2B,E,G Table S1). Using MCFO clones to label individual cells stochastically, revealed that both *Toll-6* and *kek-6* are expressed in Kenyon cells [1] (Figure 1J,K, Table S1) and DAL neurons (Figure 1M,O). This was confirmed using a DAL reporter (Figure S2H,I, Table S1). DAL neurons arborise at the SMP, overlapping with DNT-2 axonal arbours (Figure 1L, right). We also found that *Toll-6* and *kek-6* are expressed in MBONs (Figure S2). Furthermore, other *Tolls* are also expressed in the dopaminergic system. PAMs express multiple *Toll* receptors (Figure S2F,G) and all PPL1s express at least one *Toll* (Figure S2G). Similarly, Kenyon Cells and MBONs expressed various *keks* and *Tolls* (Table S1). Detailed information on cell identification is provided in Supplementary Text S1, Figure S2 and Table S1. In summary, *Toll-6* and *kek-6* are expressed in Kenyon cells, DANs, DAL and MBONs. These cells belong to a circuit required for associative learning and long-term memory, and DANs are also required for locomotion [31, 32, 35, 36, 38, 39, 75] .

Altogether, our data showed that DNT-2A neurons are glutamatergic neurons that could receive dopamine as they contacted DANs and expressed the *Dop2R* receptor, and that in turn DANs expressed the DNT-2 receptors *Toll-6* and *kek-6*, and therefore could respond to DNT-2. These data suggested that there is bidirectional connectivity between DNT-2A neurons and DANs, which we explored below.

Bidirectional connectivity between DNT-2A neurons and DANs

To verify the connectivity of DNT-2A neurons with DANs, we used various genetic tools. To identify DNT-2A output neurons, we used TransTango [76] (Figure 2A,C,E,F). DNT-2A output RFP+ arborisations were found in the superior intermediate protocerebrum (SIP), SMP, PRW (Figure 2C, Figure S3A), a subset of MB $\alpha'\beta'$ lobes, $\alpha\beta$ Kenyon cells, tip of MB $\beta'2$ (Figure 2E), DAL neurons (Figure 2F, left) and dorsal fan-shaped body layer (dFSB), centre for spatial navigation and sleep (Figure 2F, right). Consistently, these DNT-2A output neurons express *Toll-6* and *kek-6* (Supplementary Table S1). To identify DNT-2A input neurons, we used BAcTrace (Figure 2B,D)[77]. This identified octopaminergic neuron inputs at PRW (Figure S3B) and PAM neuron inputs at SMP (using *DNT-2GAL4, R58E02LexA>BAcTrace*, Figure 2D). Altogether, these data showed that DNT-2A neurons receive dopaminergic neuromodulatory inputs, their outputs include MB Kenyon cells and DAL neurons, and DNT-2 arborisations at SMP are bidirectional.

To further test the relationship between DNT-2A neurons and DANs, we first asked whether activating DNT-2A neurons could induce calcium signalling in DANs. We activated DNT-2 neurons with optogenetics (CsChrimson) and visualised calcium-dependent increase in GCaMP6 levels in PAM DANs, in live imaging experiments, and this raised GCaMP signal in PAMs (Figure 2H). This confirms that DNT-2A neurons form pre-synaptic connections with PAMs. Since DANs express DNT-2 receptors, we also asked if over-expressing DNT-2 could alter this response. DNTs/Spz proteins contain a signal peptide, an unstructured pro-domain and a conserved cystine-knot of the neurotrophin family [2, 51, 78]. Cleavage of the pro-domain releases the mature cystine-knot domain (CK). In the embryonic, larval and pupal CNS, over-expression of mature cleaved DNT-2-cystine knot (*DNT-2CK*, also known as *spz-5CK*) maintains neuronal survival and connectivity [2, 51]. Full-length DNT-2 (DNT-2FL) is cleaved spontaneously by

intracellular furins, and although DNT-2 can be found both in full-length or fully cleaved forms in vivo, it is most abundantly found cleaved [2, 3, 51]. As a result, in larvae, over-expressed *DNT-2FL* does not activate the pro-apoptotic JNK pathway and instead it activates the pro-survival ERK pathway (Foldi et al., 2017). Importantly, over-expressing *DNT-2FL* enables to investigate non-autonomous functions of DNT-2 [63]. To enable over-expressed *DNT-2* to function non-autonomously in DANs, we over-expressed *DNT-2FL* in DNT-2 neurons (Figure 2G,H). DNT-2FL did not alter the response of DANs to stimulation of DNT-2 neurons, confirming that DNT-2FL does not have an inhibitory or degenerative effect (Figure 2H). Next, we reasoned that stimulating DANs would provoke either release or production of dopamine. Since DANs express DNT-2 receptors, we asked whether increasing DNT-2 levels in DNT-2 neurons (i.e. *DNT-2>DNT-2FL*) could influence dopamine levels. We were not able to measure changes in dopamine, so we measured mRNA levels for TH instead. Using quantitative real-time PCR (qRT-PCR), we found that over-expressing *DNT2-FL* in DNT-2 neurons in adult flies increased *TH* mRNA levels in fly heads by 40%, compared to controls (Figure 2G). This showed that DNT-2 could stimulate dopamine production in neighbouring DANs.

Next, we wondered whether in turn DNT-2A neurons, that express *Dop2R*, could be modulated by dopamine. Binding of dopamine to D2-like Dop2R (also known as DD2R) inhibits adenylyl-cyclase, decreasing cAMP levels [79, 80]. Thus, to ask whether DNT-2A neurons signal via Dop2R, we activated DNT-2 neurons and tested whether *Dop2R* knock-down would increase cAMP levels. We used the FRET-based cAMP sensor, Epac1-camps-50A [81]. When Epac1-camps-50A binds cAMP, FRET is lost, resulting in decreased YFP/CFP ratio over time. Indeed, *Dop2R* RNAi knock-down in DNT-2A neurons significantly increased cAMP levels (Figure 2J), demonstrating that normally Dop2R inhibits cAMP signalling in DNT-2A cells. Importantly, this result meant that in controls, activating DNT-2A neurons caused dopamine release from DANs that then bound Dop2R to inhibit adenylyl-cyclase in DNT-2A neurons; this inhibition was prevented with *Dop2R* RNAi knock-down. Altogether, this shows that DNT-2 up-regulated TH levels, whereas dopamine inhibited cAMP in DNT-2A neurons (Figure 2I).

In summary, DNT-2A neurons are connected to DANs, DAL and MB Kenyon cells, all of which express DNT-2 receptors *Toll-6* and *kek-6* and belong to a dopaminergic as well as associative learning and

memory circuit. Furthermore, DNT-2A and PAM neurons form bidirectional connectivity (Figure 2I): EPAC and GCaMP data showed that PAMs are DNT-2 output neurons, and BAcTrace and EPAC data showed that PAMs are DNT-2 input neurons. Finally, DNT-2 and dopamine regulate each other (Figure 2I): DNT-2 increased dopamine levels, and in turn dopamine via Dop2R inhibited cAMP signalling in DNT-2A neurons. That is, an amplification was followed by negative feedback.

DNT-2 and Toll-6 maintain PAM cell survival in the adult brain

Above we showed that DNT-2 and PAM neurons are connected, so we next asked whether loss of function for *DNT-2* or *Toll-6* would affect PAMs. In wild-type flies, PAM DAN number can vary between 220-250 cells per *Drosophila* brain, making them ideal to investigate changes in cell number [82]. Furthermore, structural plasticity and degeneration can affect cell number. For example, neuronal activity and Toll-2 signalling induce neurogenesis in the adult fly brain, whereas DANs are lost in neurodegeneration models [1, 83]. Thus, to investigate whether DNT-2 could regulate structural brain plasticity, we asked whether DNT-2 influences PAM number in the adult brain. We used *THGal4; R58E02Gal4* to visualise nuclear Histone-YFP in DANs (Figure 3A) and counted automatically YFP+ PAMs using purposely developed *DeadEasy DAN* software. $DNT2^{37}/DNT2^{18}$ mutant adult brains had fewer PAMs than controls (Figure 3B). Similarly, *Toll-6* RNAi knock-down in DANs also decreased PAM neuron number (Figure 3C). DAN loss was confirmed with anti-TH antibodies, as there were fewer TH+ PAMs in $DNT2^{37}/DNT2^{18}$ mutants (Figure 3D). Importantly, PAM cell loss was rescued by over-expressing activated $Toll\text{-}6^{CY}$ in DANs in *DNT-2* mutants (Figure 3D). Altogether, these data showed that during development, DNT-2 functions via Toll-6 to maintain PAM neuron survival.

To ask whether DNT-2 could regulate dopaminergic neuron number specifically in the adult brain, we used $tubGal80^{ts}$ to conditionally knock-down gene expression in the adult. PAMs were visualised with either *R58E02LexA>LexAop-nls-tdTomato* or *THGal4; R58E02Gal4 >histone-YFP* and counted automatically. Adult specific *DNT-2* RNAi knock-down decreased Tomato+ PAM cell number (Figure 3E). Similarly, RNAi *Toll-6* knock-down in DANs in heterozygous $Toll6^{31}$ mutant flies, also decreased PAM neuron number

(Figure 3F). Furthermore, RNAi knock-down of either *Toll-6* or *DNT-2* in the adult brain caused loss of TH+ PAM neurons (Figure 3G). Thus, conditional knock-down of *DNT-2* and *Toll-6* in the adult caused dopaminergic PAM neuron loss.

To test whether cell loss was due to cell death, we visualised apoptotic cells using anti-*Drosophila* Cleave caspase-1 (DCP-1) antibodies. Adult specific *DNT-2 RNAi* knock-down increased the number of DCP-1+ cells compared to controls (Figure 3H). By contrast, *DNT-2FL* over-expression in DNT2 neurons had no effect, consistently with the fact that DNT-2FL spontaneously cleaves into the mature form [2, 3]. Importantly, *DNT-2* RNAi knock-down induced Dcp1+ apoptotic cells that were also TH+, including PAMs (Figure 3H). Thus, *DNT-2* loss of function in the adult brain induced DAN apoptosis and cell loss.

To conclude, loss of function for *DNT-2* or of its receptor *Toll-6* caused apoptosis and loss of PAMs, as seen with a nuclear reporter, anti-TH and anti-Dcp1 antibodies. Importantly, the same effect was found with sustained loss of function during development and when *DNT-2* or *Toll-6* were knocked-down conditionally in the adult only. This meant that in the adult brain, sustained PAM neuron survival depended on DNT-2 and Toll-6, and a reduction in their levels caused DAN cell loss, characteristic of neurodegeneration.

DNT-2 and its receptors are required for arborisations and synapse formation

Structural plasticity and homeostasis can also involve alterations in dendritic and axonal arborisations, and in synapse number [20]. So next we asked whether DNT-2, Toll-6 and Kek-6 could influence dendritic and axonal arbours and synapses, of neurons within their identified network, that could be analysed with high resolution: PAMs, PPL1 and DAL neurons (Figure 4C). PAM-β2β'2 neurons express *Toll-6* (Table S1), their dendrites overlap axonal DNT2 projections and can be imaged. *Toll-6* RNAi knock-down in PAM -β2β'2 (with split-GAL4 *MB301BGal4*), reduced dendrite complexity (Figure 4A). To test whether DNT-2 could alter these dendrites, we over-expressed mature *DNT-2CK*. DNT-2CK is not secreted from transfected S2 cells, but it is functional in vivo, inducing cell survival in the embryonic CNS and synaptogenesis at the NMJ [2, 51, 63]. Importantly, over-expressed *DNT-2CK* functions cell-autonomously whereas *DNT-2FL* also functions

non-autonomously, but they have the same effect [2, 51, 63]. Thus, here, we used DNT-2FL when a non-autonomous function was essential, and DNT-2CK when a cell-autonomous function was being tested. Over-expression of *DNT-2CK* in PAM -β2β'2 increased dendrite arbour complexity (Figure 4B). Thus, during development, DNT-2 and its receptor Toll-6 are required for dendrite growth and complexity in PAM neurons.

To ask whether DNT-2 could affect axonal terminals, we tested PPL1 axons. PPL1-ped neurons have a key function in long-term memory [38, 84-86], and express both *Toll-6* and *kek-6* (Table S1). Using split-GAL4 line M*B320Cgal4* to visualise PPL1 axonal arbours, RNAi knock-down of either *Toll-6*, *kek-6* or both together caused axonal misrouting away from the mushroom body peduncle (Figure 4D,D', Chi Square $p<0.05$, see Table S2). Similarly, *DNT-2FL* over-expression also caused PPL1 misrouting (Figure 4E, Chi-Square $p<0.05$, see Table S2). Thus, during development, DNT-2, Toll-6 and Kek-6 are required for appropriate targeting and connectivity of PPL1 DAN axons.

DAL neurons were identified as outputs of DNT-2 neurons expressing *kek-6* and *Toll-6* (Figure 1M,O, Figure S2H,I, Table S1). DAL neurons arborise in SMP, superior lateral protocerebrum (SLP) and anterior optic tubercle (AOTU) [36]. To visualise DAL dendritic arbours and synapses, we expressed the tagged post-synaptic density (PSD) marker *Homer-GCaMP (GFP)* [87], and focused on DAL-SLP arborisations as they can be imaged with single cell, single arbour resolution (Figure 4F-H). We first asked whether DAL dendrites might be affected during development in *DNT-2* mutants, and they were. *DNT-2^{37}/DNT-2^{18}* mutants had smaller (dendrite length) and simpler DAL dendrites (terminal points), with fewer synapses (PSD) and reduced synaptic density (PSD/total dendrite length) (Figure 4F). These data showed that DNT-2 is required in development for DAL dendrite growth and synapse formation. The volume of post-synaptic sites (PSD) increased, perhaps revealing a compensatory response to decreased synapse number (Figure 4F).

Next, we asked whether DNT-2 and Toll-6 were also required in the adult brain. Using *tubGAL80^{ts}*, we over-expressed untagged *DNT-2CK* or *DNT-2FL* in DAL neurons in the adult brain. Although this caused a mild increase in DAL dendrite size, the effect was not significantly different from controls (Figure S4A-C), meaning that increased DNT-2 levels in the adult were not sufficient to modify DAL dendrites. Synapse

number was also unaffected, but PSD volume decreased (Figure 4G), suggesting either that DNT-2 caused a decrease in PSD size, or that this was a compensatory homeostatic adjustment to raised function. By contrast, adult-specific RNAi knock-down of *Toll-6*, *kek-6* or both did not affect DAL-SLP dendritic complexity either, but it decreased Homer-GFP+ PSD number (Figure 4H) and synapse density (Figure 4H) and caused a compensatory increase in PSD size (Figure 4H). *DNT-2* mutants had a more severe phenotype in dendrite morphology than adult *Toll-6 kek-6* RNAi knock-down, perhaps revealing a function for DNT-2 throughout dendrite development or perhaps suggesting that DNT-2 could also function with other Toll and Kek receptors, as it can also bind at least Toll-7 and Kek-5 [3, 63]. In any case, these data showed that Toll-6 and Kek-6 are required for synapse formation and/or stability in DAL neurons of the adult brain.

To conclude, these data showed that DNT-2, Toll-6 and Kek-6 are required for dendrite growth, axonal targeting and synapse formation in development, and at least for synapse formation in the adult brain. The shared phenotypes from altering the levels of *DNT-2* and *Toll-6 kek-6* in dendrite and axonal arbours, and synapse formation, support their joint function in these contexts. Importantly, these findings showed that connectivity of PAM, PPL1 and DAL neurons depend on DNT-2, Toll-6 and Kek-6, in development and in the adult.

Activity-dependent synaptic remodelling requires DNT-2, Toll-6 and Kek-6

The above data showed that DNT-2, Toll-6 and Kek-6 are required for development of dendritic and axonal arbours and for synapse formation or stabilisation in development and in adults. Thus, we wondered whether they could influence activity-dependent structural plasticity or homeostasis. We first asked whether neuronal activity may influence DNT-2 levels or function. For this, we activated DNT-2 neurons with TrpA1 at 30°C, visualised tagged DNT-2GFP in adult brains and counted the number of GFP+ vesicles. In fact, activating DNT-2 neurons increased the number of tagged, fusion protein DNT-2FL-GFP+ vesicles produced (Figure 5A). To test whether neuronal activity could facilitate DNT-2 cleavage, we visualised full-length and cleaved forms from brains in western blots, using also DNT-2FL-GFP. Neuronal activation reduced the levels of full-length DNT-2FL-GFP and only cleaved DNT-2CK-GFP was present (Figure 5B).

Altogether, these data showed that neuronal activity upregulated DNT-2 levels and induced its cleavage into the mature form. We next asked what effects this may have on cell biology. Neuronal activity altered DNT-2 axonal arbours (Figure 5C). To measure the effects, and as we had shown that DNT-2 arborisations at SMP are bidirectional, we visualised PSDs in DNT-2 neurons with Homer-GFP and found that activating DNT-2 neurons increased the number of Homer-GFP+ synapses at SMP (Figure 5D). These data indicated that neuronal activity caused an increase in cleaved, mature DNT-2 and it induced synapse formation in DNT-2 neurons.

We next asked whether neuronal activity might affect dendrites and focused on DAL-SLP dendrites because they can be measured with single cell, single arbour resolution. We activated DAL neurons with TrpA1, visualised the DAL-SLP dendrite with Homer-GFP, and found that neuronal activity decreased dendrite complexity (i.e. terminal points) and size (i.e. total dendrite length, Figure 6A), thus promoting structural homeostasis. However, neuronal activity did not affect absolute synapse (PSD) number, nor synapse size (PSDs), thus resulting in increased synapse density (PSD/dendrite length, Figure 6A), meaning that it induced generation and stabilisation of synapses (i.e. structural synaptic plasticity or synaptic remodelling).

To test whether DNT-2 could mediate activity-dependent structural plasticity or homeostasis, we activated DAL neurons with TrpA1 in $DNT2^{37}/DNT2^{18}$ mutants. As we had seen before, $DNT2^{37}/DNT2^{18}$ mutants had smaller DAL dendrites and fewer synapses than wild-type, unstimulated controls (Figure 4F). When DAL neurons were activated in $DNT2^{37}/DNT2^{18}$ mutants, there was no difference in dendrite length nor synapse density with (30°C) or without (18°C control) neuronal activity (Figure 6B,D). Since dendrite length was not rescued (Figure 6D), this means that DNT-2 is not required for activity-dependent structural homeostasis, and instead is consistent with DNT-2 being required for dendrite growth. In fact, as activity decreased dendrite complexity (terminal points) even further in *DNT-2* mutants (Figure 6B,D), this means that loss of *DNT-2* function sensitised dendrites. Altogether, these data support the finding in Figure 4F that DNT-2 is required for dendrite growth. Importantly, the fact that synaptic density did not increase upon stimulation in $DNT2^{37}/DNT2^{18}$ mutants (Figure 6B,D) showed that DNT-2 is required for activity-dependent

synapse formation and remodelling. PSD volume increased in *DNT2*^{37}/*DNT2*^{18} mutants (Figure 4F), and even further with neuronal activity (Figure 6B,D), suggesting that this is a compensatory response that does not require DNT-2, in a context of synapse loss. Altogether, these data showed that synapse formation, both in development and in response to neuronal activity in the adult, depends on DNT-2.

To test whether Toll-6 and Kek-6 might also be required for such activity-dependent structural changes, we knocked them down in the adult at the same time as activating DAL neurons with TrpA1. Adult-specific *Toll-6 kek-6* RNAi knockdown did not rescue the effect of activity in dendrite size or complexity either (Figure 6C,E), meaning that Toll-6 and kek-6 are not required for activity-dependent dendrite structural homeostasis. By contrast, *Toll-6 kek-6* RNAi knockdown decreased synapse number, prevented the activity-induced synapse remodelling and instead decreased synapse density (PSD/dendrite length) (Figure 6E), meaning that Toll-6 and Kek-6 are required for activity-dependent synapse formation and remodelling. Altogether, these data show that activity-induced synaptic formation depends on Toll-6 and Kek-6.

Altogether, these data showed that neuronal activity increased levels and cleavage of DNT-2 and it induced synapse formation in DNT-2 neurons. Neuronal activity induced structural dendrite homeostasis (i.e. decreased dendrite size and complexity) and structural synaptic plasticity (i.e. increased synapse formation) in DAL neurons. Structural homeostasis of DAL neurons did not require DNT-2, Toll-6 or Kek-6 and instead data are consistent with DNT-2, Toll-6 and Kek-6 being required for dendrite growth. On the other hand, activity-induced structural synaptic plasticity depended on DNT-2 and its receptors Toll-6 and Kek-6.

Structural plasticity by DNT2 modified dopamine-dependent behaviour

Data above showed that DANs and DNT-2 neurons are functionally connected, and that loss of function for *DNT-2* or its receptors caused dopaminergic neuron loss, altered DAN arborisations and caused synapse loss, altogether modifying circuit connectivity. Next, to measure the effect of such circuit modifications on behaviour, we used dopamine-dependent behaviours as readout.

Startle-induced negative geotaxis, also known as the climbing assay, requires dopamine and specifically PAM neuron function [88, 89]. Thus, we tested the effect of *DNT-2* or *Toll-6 kek-6* loss of function in climbing. Neither *DNT-2*^{37}/*DNT-2*^{18} mutants nor flies in which *DNT-2* was knocked-down in DNT-2 neurons in the adult, could climb as well as controls (Figure 7A). Similarly, when *Toll-6* and *kek-6* were knocked-down with RNAi in the adult in either Toll-6 neurons or in PAM neurons, flies could not climb well either (Figure 7B). Importantly, over-expressing activated Toll-6^{CY} in DANs could rescue the locomotion deficits of *DNT-2* mutants, showing that DNT-2 functions via Toll-6 in this context (Figure 7C). Interestingly, both loss and gain of function for DNT-2 also caused seizures (Figure S5). We also tracked freely moving flies in an open arena [90], and compared to controls, adult flies over-expressing *DNT2-FL* walked faster (Figure 7D). Activating DNT-2 neurons with TrpA1 had the same effect (Figure 7E), consistently with the fact that activating neurons increased DNT-2 production (Figure 6B). Thus, dopamine-dependent locomotion depended on DNT-2, Toll-6 and Kek-6 function.

Next, as dopamine is the essential neurotransmitter for appetitive learning [31, 32], we asked whether DNT-2 might influence associative reward learning and long-term memory. Wild-type control or *DNT2*^{18}/*DNT-2*^{37} starved mutant flies were trained to pair an odour with sugar vs. a second odour with only water. Flies were tested in the absence of sugar and their choice of either conditioned odour (CS+) or un-conditioned odour (CS-) was recorded as a measurement of appetitive long-term memory, 24h after training (as in [37, 91]). Remarkably, *DNT2*^{18}/*DNT-2*^{37} mutants had impaired appetitive long-term memory (Figure 7F). Conversely, over-expressed *DNT-2FL* in DNT-2 neurons in adults enhanced appetitive long-term memory (Figure 7G). Moreover, simply activating DNT-2 neurons in the adult with TrpA1 was sufficient to enhance appetitive long-term memory (Figure 7H). This was consistent with the finding that neuronal activity increased DNT-2 levels and cleavage. These data demonstrate that DNT-2 is required for and can promote learning and long-term memory.

In summary, using dopamine-dependent locomotion and long-term memory as behavioural readouts, we could show that alterations in DNT-2, Toll-6 and Kek-6 levels that caused structural phenotypes in PAMs, PPL1 and DAL neurons also modified behaviour.

DISCUSSION

Understanding the link between structural circuit modification and behaviour is key to understand how the brain works and how to maintain brain and mental health. Neuronal activity and experience could elicit structural brain change via Toll receptors, which can regulate a wide range of cellular processes [1]. On the other hand, neuromodulators like dopamine assign a value to otherwise neutral stimuli, in an experience-dependent context, labelling neural circuits involved. We had previously observed that Toll-6+ neurons express the dopaminergic neuron marker, TH [3]. Thus, here we explored whether a functional link between Toll-6 and dopamine could drive activity-dependent circuit plasticity and behavioural modification, using dopamine-dependent behaviours as readout (Figure 8A). Here we showed that DNT-2 and its receptors Toll-6 and Kek-6 are linked to the dopaminergic circuit, and that DNT-2 and dopamine regulate each other (Figure 8A,B). Neuronal stimulation resulted in an up-regulation of both DNT-2 and dopamine, and in turn DNT-2 with Toll-6 and Kek-6 drove structural remodelling of a dopaminergic circuit, modifying behaviour (Figure 8A). Altering the levels of DNT-2, Toll-6 and Kek-6 altered cell number, neurites and synapses in DAL and DAN neurons, and these circuit modifications modulated the dopamine-dependent behaviours locomotion, learning and long-term memory (Figure 8C). We used neuronal activation as a proxy for experience, but the implication of our findings is that experience would similarly drive the structural modification of circuits labelled by neuromodulators (Figure 8A,B). Furthermore, our findings show that structural brain plasticity and degeneration are two aspects of a shared process that normally keeps the healthy brain in balance (Figure 8C). Whereas gain of function for *DNT-2* and *Toll-6* promoted structural plasticity, their deficits caused neurodegeneration, prevented structural plasticity and impaired behaviour. Finally, we have shown that structural plasticity depends on a novel molecular mechanism involving a neurotrophin ligand working with a Toll and a kinase-less Trk-family receptor that modify a neuromodulatory circuit (Figure 8A).

DNT-2A and DANs form bidirectional connectivity that modulates both DNT-2 and dopamine (Figure 8A). Activating DNT-2 neurons increased the levels and cleavage of DNT-2, which increased levels of TH. This initial amplification in turn resulted in the inhibition of cAMP signalling in DNT-2 neurons via

Dop2R. This implied that activation of DNT-2 neurons resulted in the release of dopamine from output neurons, which then lead to inhibitory signalling in DNT-2A cells – that is, initial increase followed by negative feedback. This negative feedback could drive a homeostatic reset of both DNT-2 and dopamine levels, that could be important for normal brain function. In fact, in humans, dopamine and neurotrophins (NTs) are functionally linked, and alterations in both underlie psychiatric disorders and neurodegenerative diseases [92-94].

Structural plasticity and neurodegeneration are two manifestations of a shared process that depends on DNT-2, Toll-6 and Kek-6 (Figure 8C). DNT-2 induced structural plasticity, as it increased dendritic complexity, altered axonal targeting and up-regulated TH levels, and neuronal activity up-regulated DNT-2 levels, triggered DNT-2 cleavage, and induced structural synaptic plasticity, which depended on DNT-2. Conversely, loss of function for *DNT-2*, *Toll-6* and *kek-6* caused phenotypes of neurodegeneration, including apoptosis, neuronal loss, decrease in dendritic complexity, impaired fasciculation and targeting, and synapse loss. These phenotypes support previous findings that Toll-6 functions as a neurotrophin receptor for DNT-2, promoting cell survival and connectivity in embryos [3]; that Toll-6 can promote cell survival in embryos and larvae [2][3]; that Toll-2 is neuroprotective [1]; and that Toll-6 and Kek-6 together promote synaptogenesis at the larval NMJ [63]. Neuronal activity caused structural homeostasis in dendritic arbours and structural synaptic plasticity and remodelling. Our data showed that, in the context analysed, DNT-2, Toll-6 and Kek-6 were not required for activity-dependent dendrite structural homeostasis, but instead were required for dendrite growth and structural synaptic plasticity. This is consistent with their functions promoting axonal arbour growth and synapse formation at the NMJ [63]. It also suggests that other mechanisms regulate structural dendrite homeostasis, which could still include other Spz family ligands, Tolls and Keks. There are six *spz*, nine *Toll* and six *kek* genes in *Drosophila* [62, 63, 68, 95], and at least seven Tolls and three adaptors are expressed in distinct but overlapping patterns in the brain [1]. Different Tolls could be distributed in different neuronal types, or sub-cellular locations (e.g. dendrites vs. axons), and could potentially drive distinct cellular outcomes. The

combinatorial complexity of DNTs, Tolls and Keks opens the possibility for a fine-tuned regulation of structural circuit plasticity and homeostasis in the brain.

We showed that the structural circuit modifications by DNT-2 with Toll-6 and Kek-6 modulated behaviour, using dopamine-dependent behaviours are readout. Dopamine is required for locomotion in *Drosophila*, and it is required specifically in PAMs for climbing [30, 88, 89]. Importantly, *Drosophila* models of Parkinson's Disease reproduce the loss of DANs and locomotion impairment found in human patients [30, 83, 88, 89]. We showed that loss-of function for *DNT-2, Toll-6* and *kek-6* caused DAN loss and impaired locomotion, and DNT-2 gain of function and neuronal activation of DNT-2 neurons enhanced locomotion, consistently with the fact that neuronal activity increased DNT-2 levels. Dopamine is also required for associative reward learning and long-term memory [31, 32]. This requires PAM, PPL1 and DAL neurons and their connections to Kenyon Cells and MBONs, in *Drosophila* [32, 35, 36, 39]. We showed that: 1, DNT-2 neurons are connected to all these neuron types, which also express *Toll-6* and *kek-6*; 2, *DNT-2* mutants had fewer PAMs, fewer DAL synapses and impaired long-term memory; 3, that neuronal activity remodelled DAL synapses, and this required *DNT2, Toll-6* and *kek-6*; 4, that stimulation of DNT-2 neurons increased long-term memory; 5, and that and over-expression of *DNT-2* increased TH and long-term memory. Altogether, these data demonstrate that structural circuit changes caused by altering the levels of DNT-2, Toll-6 and Kek-6 modified dopamine-dependent behaviours, providing a direct link between structural brain change and behavioural modification.

DNT-2 differs from DNT-1 and Spz-1, as it carries out the same functions when it is over-expressed in cystine-knot or full-length forms. DNTs/Spz-family proteins contain a signal peptide, an unstructured pro-domain and a conserved neurotrophin cystine-knot [2, 78]. However, while Spz-1 is cleaved by a Ser-protease cascade [78, 96], DNT-1 and DNT-2 are not, and they are cleaved by furins instead [2]. DNT-2FL is spontaneously cleaved by furins to release the mature DNT-2CK form in all contexts tested, i.e. baculovirus infected insect cells, S2 cells and in vivo in flies [2, 3]. DNT-2 can be found full-length or fully cleaved in vivo, but it is most abundantly cleaved, and only promotes cell survival [2, 3, 51]. By contrast, in vivo, DNT-1 can be found either as full-length, mature or as an intermediate cleavage product form that retains most of

the pro-domain and can promote apoptosis [2, 3, 51]. In S2 cells, transfected cleaved DNT-2CK is not secreted, but nevertheless, it is functional in vivo. Over-expressed cleaved *DNT-2CK* promotes cell survival in embryos [2, 51] and over-expressed *DNT-2CK* induces synapse formation in larvae [63]. Similarly, over-expressed mature *spz-1C106* can rescue the *spz-1*-null mutant phenotype [97] and over-expressed *DNT-1CK* can rescue the *DNT-1* mutant phenotype [51]. Importantly, over-expressed *DNT-2CK* functions cell-autonomously whereas *DNT-2FL* also functions non-autonomously, but they have the same effect promoting cell survival and synaptogenesis [2, 51, 63]. Thus, over-expressed DNT-2FL is naturally cleaved and secreted and has non-autonomous as well as cell-autonomous functions. Instead, over-expressed *DNT-2CK* is not secreted and functions cell autonomously. DNT-2FL and DNT-2CK consistently have neuro-protective functions promoting cell survival, neurite growth and synaptogenesis [2, 51, 63]. Furthermore, DNT-2 is a retrograde factor at the NMJ, as transcripts are located post-synaptically, and over-expressed DNT-2FL-GFP in muscle is taken up by motorneurons [51, 63]. Our findings show that in the analysed circuits of the adult brain, over-expressed *DNT-2* is neuroprotective and induces structural plasticity as: (1) DNT-2FL did not induce apoptosis nor inhibitory signalling; (2) DNT-2CK increased dendritic complexity; (3) both DNT-2FL and CK had the same effect in PPL1 axons and in DAL synapses; (4) DNT-2FL increased TH expression non-autonomously; and (5) DNT-2FL increased locomotion and long-term memory.

Toll receptors in the CNS can function via ligand dependent and ligand-independent mechanisms. Here, we provide evidence that the function of Toll-6 and Kek-6 in structural circuit plasticity depends on DNT-2: 1, Loss of function for *DNT-2, Toll-6* and *kek-6* caused the same phenotypes of apoptosis and loss of PAMs, alterations in arborisations, loss of synapses, increased PSD volume and impaired locomotion. 2, Gain of function for *DNT-2* caused the opposite phenotypes compared to loss of *Toll-6 kek-6* function, including increased dendritic complexity, decreased PSD volume and increased locomotion. 3, Over-expression of *activated Toll-6*^{CY} could rescue the loss of PAM DANs of *DNT-2* mutants. 4, Over-expression of *activated Toll-6*^{CY} could rescue the locomotion impairment of *DNT-2* mutants. Thus altogether, our data show that DNT-2 regulates structural plasticity in the adult brain via Toll-6 and Kek-6.

This work has uncovered a novel mechanism of structural brain plasticity, involving a NT ligand functioning via a Toll and a kinase-less Trk-family receptor in *Drosophila*. Together, they regulate cell survival, neurite growth, connectivity, synaptogenesis and behaviour - from development to the adult brain and in response to neuronal activity. In mammals, these functions are regulated by NTs functioning via Trk, $p75^{NTR}$ and Sortilin receptors instead. Importantly, alterations in NT function underlie psychiatric, neurologic and neurodegenerative brain diseases [9-11, 52, 53, 65, 70, 98]. Intriguingly, in mammals, kinase-less isoforms of Trk receptors regulate CaMKII and dendrite growth and have been linked to neurodegenerative and psychiatric disorders [67, 99-104]. Our findings expand the evidence that despite differences in receptors, equivalent functions are carried out by mammalian NTs and DNTs in *Drosophila* further demonstrating the evolutionary conservation of the NT protein family. We also showed that *DNT-2* over-expression upregulated *TH* expression. Similarly, mammalian NTs promote dopamine release and the expression of DA receptors [93, 105]. Importantly, we showed that DAN cell survival is maintained by DNT-2 in *Drosophila.* Similarly, DAN cell survival is also maintained by NT signalling in mammals and fish [92, 106]. Such deep evolutionary conservation suggests that brain function requires a close relationship between NT and dopamine signalling. In the course of evolution *Drosophila* and mammalian NTs may have evolved to use different receptor types to elicit equivalent cellular outcomes. Ultimately, these result in the regulation of DAN cell number, cell shape and synaptogenesis to enable neural circuit formation and modification. However, two interesting facts remain: 1, Kek-6 is a kinase-less Trk-family receptor lacking a tyrosine kinase domain. In the mammalian brain, Trk-B has around 100 isoforms encoding at least 10 distinct proteins, not all with a kinase domain and most of them of unknown function [107, 108]. Kinase-less Trk isoforms (e.g. TrkB-T1, TrkC-T1, TrkB-T-Shc) can function as ligand sinks and dominant negative forms and they can also function independently of full-length Trks, signalling via PLCγ, CaMKII and Rho1, influencing calcium levels, the cytoskeleton, growth cone extension and the mode of dendritic growth [67, 103, 109]. Importantly, TrkB-T1 is the most abundant TrkB isoform in the adult human brain, can alter dendrites and is linked to psychiatric disorders, e.g. depression [67, 103]. Thus, evolutionarily conserved functions of kinase-less Trks could be more important for structural brain plasticity and function than

previously thought. 2, In cell culture, human neurotrophins BDNF and NGF can induce signalling from TLRs [2]. This means that either BDNF directly binds TLRs, or that binding of BDNF to a Trk or p75 receptor enables TLR signalling [2]. Either way, this strongly suggests a functional relationship between NTs and TLRs exists also in humans. Importantly, TLRs can regulate non-immune functions in the CNS including cell survival, death and proliferation, neurogenesis, neurite growth and collapse, learning and memory [58]. TLRs are linked to psychiatric disorders (e.g. depression), neurodegenerative diseases and stroke [58, 110, 111]. Intriguingly, GWAS have revealed involvement of TLRs in various brain conditions and potential links between neurotrophins and TLRs in, for example, major depression [112-115]. It is compelling to find out whether the relationship uncovered here between dopamine, NTs, TLRs and kinase-less Trks operates also in humans.

To conclude, we have shown that neuronal activity results in an initial amplification of both DNT-2 and TH levels, which then regulate each other homeostatically. Dopamine labels the circuits engaged and DNT-2, a growth factor, with its receptors Toll-6 and Kek-6, drives structural synaptic plasticity in these circuits leading to the modulation of behaviour, including locomotion and memory. If there is a deficit for DNT-2 or its receptors, this causes neurodegeneration and dopamine-dependent behavioural deficits including impaired locomotion and long-term memory. Thus, DNT-2, Toll-6 and Kek-6 regulate the balance between structural plasticity and degeneration in a neuromodulatory circuit, modifying behaviour. Our data provide a direct link between activity-dependent structural modification of a neuromodulatory circuit and the resulting behaviour, by an identified molecular mechanism. An implication of this study is that subjective experience could similarly result in the structural modification of neural circuits labelled by neuromodulators, driving behavioural modification. Thus, as experience and behaviour are sources of structural brain change, this has profound implications for understanding brain function and health. A similar mechanism involving the combination of NTs functioning together with TLRs and kinase-less Trks in dopaminergic circuits could help understand brain and mental health in humans.

ACKNOWLEDGEMENTS

We thank our lab for discussions and Carolina Rezaval and Thomas Riemensperger for comments on the manuscript; Carolina Rezaval for advice and sharing kit for behaviour experiments; Reinhard Wolf, Martin Heisenberg, Vincent Crozet and Scott Waddell for training on learning and memory tests, for sharing kit and designs, helping us get equipped and for advice; Serge Birman, Ann-Shyn Chiang, Ron Davis, André Fialá, Carolina Rezaval for flies; DSHB (Iowa) for antibodies; AddGene for plasmids; Bloomington Stock Centre for *Drosophila* stocks. This work was funded by Marie-Curie Sklodowska Post-Doctoral fellowship to J.S.; Science Without Borders-CAPES PhD Studentship BEX 13380/13-3 to SUB; BBSRC Project Grants BB/R00871X/1 and BB/P004997/1 to A.H.; and Wellcome Trust Investigator Award 223197/Z/21/Z to A.H.

AUTHOR CONTRIBUTIONS

J.S. designed and executed experiments, analysed data and wrote manuscript; S.U-B, G.L, D.S, M.M. executed experiments; M.G.F, S.C. developed tools; F.R-C analysed data; D.K.,G.J,A.H. supervised; A.H. conceived and directed the project, analysed data, wrote manuscript. All authors contributed to improvements to the manuscript.

DECLARATION OF INTERESTS

The authors declare that they have no conflict of interest.

MATERIALS AND METHODS

Genetics

Mutants: *DNT2*^{37} and *DNT2*^{18} are protein null [63]. *Toll6*^{31} is a null mutant allele [3]. **Driver lines:** *DNT2-Gal4* is a CRISPR/Cas9-knock-in allele, with GAL4 at the start of the gene (this work, see below). *Toll-6-Gal4* was generated by RMCE from *MIMIC Toll-6*^{MIO2127}*; kek6-Gal4* from *MIMIC Kek6*^{MI12953} [1, 63]. MB320C-Gal4 (BSC68253), MB301B-Gal4 (BSC68311), R58E02-Gal4 (BSC41347), MB247-Gal80 (BSC64306), R58E02-LexA (BSC52740), R14C08-LexA (BSC52473) were from the *Drosophila* Bloomington Stock Centre (BSC). Dop1R1-

LexA, Dop2R-LexA, Gad-LexA were kindly provided by Yi Rao; TH-LexA (gift of Ron Davis), Tdc2-LexA and Trh-LexA (gift of Carolina Rezaval), TH-Gal4,R58E02-GAL4 (gift of Serge Birman); G0431-Gal4, VT49239 nls LexA (DAL LexA) (gifts from Ann-Shyn Chiang). **Reporter lines:** *UAS-CD8::GFP,* for membrane tethered GFP; *UAS-histone-YFP*, for YFP-tagged nuclear histone; *UASflybow1.1*, constant membrane tethered expression; *13xLexAop-nls-tdTomato,* nuclear Tomato; *UASCD8::RFP, LexAopCD8::GFP* (BSC32229), for dual binary expression; *UAS-homer-GCaMP* for post-synaptic densities (gift of André Fialá). **For connectivity***: UAS-DenMarkRFP, UAS-Dsyd1GFP* (gift of Carolina Rezaval); TransTango: *yw* {*UAS-myrGFP,QUAS-mtdTomato-3xHA}attP8; Trans-Tango@attP40* (BSC77124); BAcTrace 806 *(w;LexAop2-Syb::GFP-P10(VK37) LexAop-QF2::SNAP25::HIVNES::Syntaxin(VK18)/CyO; UAS-B3Recombinase (attP2) UAS<B3Stop<BoNT/A (VK5) UAS<B3Stop<BoNT/A(VK27) QUAS-mtdTomato::HA/TM2*): **MCFO clones**: *hs-FLPG5.PEST;; 10xUAS (FRT.stop) myr::smGdP-OLLAS} 10xUAS (FRT.stop) myr::smGdP-HA 10xUAS (FRT.stop) myr::smGdP-V5-THS-10xUAS (FRT.stop) myr::smGdP-FLAG* (BSC64086). **Live imaging:** cAMP sensor: *UAS-Epac1-camps-50A* (BSC25408); Ca^{2+} sensor: *13XLexAop2-IVS-GCaMP6s-p10 su(Hw)attP1 (BDSC44272), 13XLexAop2-IVS-GCaMP6s-p10 su(Hw) attP5* (BSC44590). **Optogenetic activation:** *20x UAS V5 Syn CsChrimson td tomato* (B. Pfeiffer). **UAS gene over-expression**: *UAS-DNT2CK, UAS-DNT2FL-GFP, UAS-DNT2-FL-47C* [2, 3]. **UAS-RNAi knockdown:** *UAS-DNT2RNAi* (VDRC49195), *UAS-Toll6RNAi* (VDRC928), y^1v^1*; UAS-Toll6RNAi[Trip.HMS04251]* (BSC 56048*), UAS-kek6RNAi* (VDCR 109681), y^1v^1*; UAS-Dop2R-RNAi[TRiP.HMC02988](*BSC50621).

Molecular biology

DNT-2GAL4 was generated by CRISPR/Cas9 enhanced homologous recombination. 1 kb long 5' and 3' homology arms (HA) were amplified by PCR from genomic DNA of wild type flies, using primers for 5'HA: atcgcaccggtttttacaggcaccccatgtctga containing AgeI cutting site and cttgacgcggccgcTGTCAATTCATTCGCCGTCGAT containing NotI cutting site. 3'HA primers were: tattaggcgcgccATGACAAAAAGTATTAAACGTCCGCCC containing AscI cutting site and tactcgactagtgaagcacacccaaaatacccagg containing SpeI cutting site. HAs were sequentially cloned by conventional cloning into pGEM-T2AGal4 vector (Addgene #62894). For gRNA cloning, two 20 nucleotide

gRNA oligos (gtcGACAAGTTCTTCTTACCTATG and aaacCATAGGTAAGAAGAACTTGTC) were designed using Optimal Target Finder. BbsI enzyme sites were added: gtc(g) at the 5' end of sense oligo, and aaac at the 5' end of the antisense oligo. gRNA is located at 41 bp downstream of the start codon of DNT-2 within the first coding exon. The gRNA was cloned into pU6.3 using conventional ligation. The two constructs were injected in Cas9 bearing flies and red fluorescent (3xP3-RFP) transformants were selected and balanced, after which 3xP3-RFP was removed with CRE-recombinase.

qRT-PCR

qRT-PCR was carried out from 20 whole adult fruit-fly heads, frozen in liquid nitrogen before homogenising in 50 μl Trizol (Ambion #AM9738), followed by a stand RNA extraction protocol. RNA was treated with DNase treatment (ThermoFisher # AM1906) to remove genomic DNA. 200 ng of RNA was used for cDNA synthesis following Goscript Reverse Transcriptase (Promega #237815) protocol. Sample was diluted 1:4 with Nuclease free H_2O. Standard qPCR was performed with SensiFast syb Green Mix (Bioline #B2092020) in ABI qPCR plate (GeneFlow #P3-0292) and machine. To amplify TH mRNA the following primers were used: TH-F: CGAGGACGAGATTTTGTTGGC and TH-R: TTGAGGCGGACCACCAAAG. GAPDH was used as a housekeeping control. Reactions were performed in triplicate. Specificity and size of amplification products were assessed by melting curve analyses. Target gene expression relative to reference gene is expressed as value of $2^{-\Delta\Delta Ct}$ (where Ct is the crossing threshold).

Conditional expression

Multiple Colour Flip Out clones: *DNT2-Gal4, Toll6-Gal4* and *kek6-Gal4* were crossed with *hsFLP::PEST;;MCFO* flies, female offspring were collected and heat-shocked at 37°C in a water bath for 15 mins, then kept for 48h at 25°C before dissecting their brains. **TransTango:** DNT2-Gal4 or Oregon female virgins were crossed with TransTango males, progeny flies were raised at 18°C constantly and 15 days after eclosion, female flies were selected for immunostaining. **Thermogenetic activation with TrpA1:** Fruit-flies were bred at 18°C from egg laying to 4 days post-adult eclosion, then shifted to 29°C in a water bath for

24h followed by 24h recovery at room temperature for over-expressed DNT-2FL-GFP; for the other experiments, after breeding as above, adult flies were transferred to an incubator at 30°C, kept there for 24h and then brains were dissected. **Conditional gene over-expression and RNAi knockdown:** Flies bearing the temperature sensitive GAL4 repressor tubGal80^{ts} were kept at 18°C from egg laying to adult eclosion, then transferred to 30 °C incubator for 48h for Dcp-1+ and cell counting experiments and for 120h for TH+ cell counting.

Immunostainings

Adult fruit-fly female brains were dissected (in PBS), fixed (in 4% para-formaldehyde, room temperature, 20-30min) and stained following standard protocols. Primary antibodies and their dilutions were as follows: Mouse anti-Brp (nc82) 1:10 (DSHB); Rabbit anti-GFP 1:250 (Thermofisher); Mouse anti-GFP 1:250 (Thermofisher); Chicken anti-GFP 1:500 (Aves); Rabbit anti-FLAG 1:50 (Sigma); Mouse anti-V5 1:50 (Invitrogen); Chicken anti-HA 1:50 (Aves); Rabbit anti-VGlut 1:500 (gift of Hermann); Mouse anti-TH 1:250 (Immunostar); Rabbit anti-TH 1:250 (Novus Biologicals); Rabbit anti-DsRed 1:250 (Clontek); Mouse anti-ChAT4B1 1:250 (DSHB); Rabbit anti-5-HT 1:500 (Immunostar); Rabbit Anti-DCP-1 1:250 (Cell Signalling). Seconday antibodies were all used at 1:500 and all were from Thermofisher: Alexa Flour 488 Goat anti-mouse, Alexa Flour 488 donkey anti-rabbit, Alexa Flour 488 Goat anti-rabbit (Fab')2, Alexa Flour 488 Goat anti-chicken, Alexa Four 546 Goat anti-rabbit, Alexa Four 546 Goat anti-mouse, Alex Four 647 Goat anti-rabbit, Alex Four 647 Goat anti-mouse.

Microscopy and Imaging

Laser scanning confocal microscopy. Stacks of microscopy images were acquired using laser scanning confocal microscopy with either Zeiss LSM710, 900 or Leica SP8. Brains were scanned with a resolution of 1024x1024, with Leica SP8 20x oil objective and 1 μm step for whole brain and DCP-1 stainings, 40x oil objective and 1 μm step for central brain. Resolution of 1024x512 was used for analysing PAM clusters with 0.96 μm step for cell counting; 0.5 μm step for neuronal morphology; and 63x oil objective with 0.5μm step

for neuronal connections. Acquisition speed in Leica SP8 was 400Hz, no line averaging. Resolution of 3072x3072 was used for single image analysis of synapses, using Zeiss LSM900 and Airyscan acquisition with 40x water objective speed 6, and average 4, or with 1024x512, with 40x oil lens 2x zoom and 0.35μm step. TH counting in PAM were scanned with Zeiss 710 with a resolution 1024x1024, 40x oil objective, step 1 μm, speed 8.

Optogenetics and 2-photon microscopy:

1. Real time GCaMP imaging. To ask whether stimulation of DNT-2 neurons could activate output PAM neurons, DNT-2 neurons were depolarised using DNT-2GAL4>UAS-CsChrimson and activation of PAM neurons was tested using R58E02LexA driving expression of the LexAopGCaMP6s calcium reporter, *ex vivo*. 1-3 day-old R58E02LexA DNT2Gal4 UASCsChrimson LexAopGcamp6s flies were collected and separated into two groups. One group was fed normal food and the second group were fed freshly prepared food containing 50μM all-trans retinal, vials were wrapped with foil paper in complete darkness, for at least 3 days prior to experiments. Flies were put on ice and brains were dissected in adult hemolymph-like solution (103mM NaCl, 3mM KCl, 5mM N-Tris, 10mM trehalose, 10mM glucose, 7mM sucrose, 26mM $NaHCO_3$, 1mM NaH_2PO_4, 1.5mM $CaCl_2$, 4mM $MgCl_2$). Because of the sensitivity of GCaMP6s, brains were left in the dark for 15-20min after mounting on poly-L-lysine coated slides to prevent any potential brain movements, and subsequently were processed for imaging. The settings for GCaMP6s recording were set according to [116] at a frame rate of 10 Hz, at 925nm using an Olympus FVMPE-RS two-photon microscope with an FV30-FGR filter. To activate CsChrimson optogenetically, each fly was stimulated using a sapphire laser at 588nm, targeting the laser onto DNT-2 projections in the SMP region for 20s. The recording started 10s before the stimulation and lasted 1min after 20s stimulation.

GCaMP image analysis was performed using ImageJ. A region of interest (ROI) was defined where GCaMP intensity was seen to change in response to stimulation. Fluorescence intensity within the ROI was measured across each frame and background fluorescence (F0) was determined as the average of 5 frames before stimulation. Normalised fluorescence intensity dF/F0(GcaMP6s) was calculated for the ROI for each frame after stimulation. Graphs were produced with GraphPad Prism.

2. Epac1 FRET 2-photon imaging. To test whether DNT-2 neurons can respond to dopamine via the Dop2R inhibitory receptor, we used the cAMP sensor Epac1 and 2-photon confocal microscopy. Epac1 is FRET probe, whereby data are acquired from CFP and YFP emission and lower YFP/CFP ratio reveals higher cAMP levels. DNT-2Gal4 flies were crossed to UAS-CsChrimson UAS Epac1 flies, to stimulate DNT-2 neurons and detect cAMP levels in DNT2 neurons. 1-3 day-old DNT2Gal4>UASCsChrimson, UAS Epac1 flies were collected and separated in two groups. Flies bearing DNT2Gal4 UASCsChrimson UAS Epac1 UASDop2RRNAi were fed on 50μM all-trans retinal food for at least 3 days prior to imaging and kept in constant darkness prior to the experiment.

Optogenetic stimulation of fly brains expressing CsChrimson in DNT-2 neurons was carried out using a sapphire 588nm laser, in a 2-photon confocal microscope. For acquisition of YFP and CFP data from Epac1 samples, a FV30-FYC filter was applied, using a 925nm laser for both YFP and CFP imaging. The stimulation laser was targeted onto DNT-2 neuron projections in SMP region for 20s. Acquisition ROI was at DNT-2A cell bodies with a frame rate of around 10Hz. The first acquisition started 10s before the 20s stimulation and consequential acquisition was done every 30s for 10 cycles.

Image analysis of Epac data was carried out using ImageJ. The two channels (YFP and CFP) were separated, and the ratio of YFP/CFP for each pixel was calculated using the ImageJ>Image Calculator by diving YFP channel by CFP channel. The obtained result of YFP/CFP ratio was saved and the mean ratio of YFP/CFP in the ROI was calculated for each time point and 11 time points were used. The 11 values represent the ratio of YFP/CFP change in the cell body upon stimulation, with 30s interval and repeated 10 times.

Automatic cell counting with DeadEasy plug-ins: To automatically count cell number labelled with nuclear reporters (e.g. Histone-YFP, nls-tdTomato) and Dcp-1+ cells, we adapted the DeadEasy Central Brain ImageJ plug-in [1]. DeadEasy automatically identifies and counts cells labelled with nuclear reporters in 3D stacks of confocal image in the adult central brain. Brains expressing these reporters were dissected, fixed and scanned without stainings. DeadEasy Central Brain was used with threshold set to 75.

To count the TH labelled PAMs, we purposely developed a newly plug-in called DeadEasy DAN. Since TH-stained images had Poisson noise, a median filter was used to reduce noise, without having large losses at the edges. Then, given that cell walls of irregular intensity are frequently encountered, a 3D morphological enclosure was performed. Since each cell is identified as a dark area surrounded by pixels of higher intensity and that, in the background, due to noise, it is also possible to find local minima that can be incorrectly identified as cells, all very dark pixels were assigned a value of zero. To mark each cell, each chasm in the image was found using a 3D extended h-minimal transform. As more than one local minimum can be found within each cell, which would result in counting a cell multiple times, a 3D inverse dome detection was performed, and then labelled. Thus, each inverse dome was used as a seed to identify each cell. Once the seeds were obtained, a 3D watershed transformation was performed to recover the shape of the cells. Finally, a colour palette was used to visualize each cell more easily. DeadEasy DAN is accurate in controls and mutants, but less accurate with RNAi knock-down genotypes, for which it was not used and TH+ cells were counted manually instead, assisted by the imageJ cell counter.

Dendrite analysis with Imaris: To analyze dendritic complexity, image data were processed with Imaris using the "Filament Autodetect" function with the default algorithm and autopatch function. Setting of the threshold was consistent within the same experiment: the largest or smallest diameter of the dendrite, same threshold for background substation, local contrast. Number of dendritic branches, dendritic segments, dendritic branch points and dendritic terminal points were collected to compare the difference between the groups.

PSD analysis with Imaris: To analyse the number and volume of Homer-GCaMP GFP+ post-synaptic densities (PSD), image data were processed with the Imaris-Spot function. Setting of the threshold was consistent across experiments.

Brain registration and Nblast: DNT-2 single neurons imaged from DNT-2GAL4>MCFO brains were used for brain registration, following the protocol described in [117]. JFRC2 was chosen as the template for DNT-2 neuron registration. Leica SP8 lasering confocal microscopy was used for image acquisition with 20x oil objective, 1024x512, Zoom 0.91 step 1µm, 218 total frames. Fiji with CMTK plug-ins were applied for brain

registration. The reformatted brains were opened in Fiji-single neuron trace to obtain the approximate neuron trace of DNT-2 neurons. The obtained neuron traces were uploaded to Nblast to find similar neurons [71].

Behaviour

1. Startle induced negative geotaxis Assay was carried out as described in [89]. Groups of approximately 10 male flies of the same genotype were placed in a fresh tube one night before the test, after which flies were transferred to a column formed with two empty tubes 15cm long and 2cm and then habituated for 30mins. Columns were tapped 3-4 times, flies fell to the bottom and then climbed upwards. Multiple rounds of testing were performed 3-7 times in a row per column. The process was filmed and films were analysed. Flies were scored during the first 15s after the tapping, and those that climbed above 13cm and those that climbed below 2cm were counted separately. Results given are mean ± SEM of the scores obtained with ten groups of flies per genotype. The performance index (PI) is defined as $1/2[(n_{tot} + n_{top} - n_{bot})/n_{tot}]$, where n_{tot}, n_{top}, and n_{bot} are the total number of flies, the number of flies at the top, and the number of flies at the bottom, respectively. The assay was carried out at 25°C, 55% humidity. Flies with tubGal80^{ts} to conditionally overexpress or knock-down, flies were shifted from 18 to 30°at eclosion and kept for 5 days at 30°C to induce Gal4. Experiments were carried in an environmental chamber at 31°C, 60% humidity or in a humidity and temperature controlled behaviour lab always kept at 25°C.

2. Locomotion in an open arena: For loss and gain of function experiments, fruit-flies were raised at 18°C until eclosion, then transferred to 30°C for 5 days and split into groups of 5 flies per tube one day before the locomotion test. Using an aspirator, three flies were transferred into a well of a multi-well plate with diameter 24mm, through a small hole in the transparent lid of the plate. They were then placed on the white LED light pad, where they were habituated for 30 mins before filming. A camera was placed on a tripod inside an environmental chamber kept at 30°C, 60%, where groups of flies within the wells on the light pad, were filmed. For thermoactivation or inhibition with *DNT2-Gal4*, flies were raised at 18°C and kept at 18°C for 7-9 days post-eclosion. After habituation at 18°C for 20 mins flies in multi-well plates were

transferred to the 30°C environmental chamber, left for 10 mins to activate TrpA1 and then filmed for 10 mins. Fly locomotion in films was analysed in 5min (300 seconds) of filming, using Flytracker software [90].For "speed" only frames when flies were moving above 4 mm/s (which corresponds to two body lengths), were used.

3. Appetitive long term memory test: Mixed sex population of 4-8 day old flies raised at 25 °C were tested together in memory assays for Cantons/Oregon and *DNT2*^{37}/*DNT2*^{18} mutants. Appetitive memory was tested according to Krashes and Waddell [91]. Odors used in conditioning were 3-octanol (Sigma-Aldrich # 218405) (6µL in 8mL mineral oil Sigma-Aldrich #330760) with 4-methylcyclohexanol (Sigma-Aldrich # 153095) (7µL in 8mL mineral oil). Groups of ~80 flies were kept in a 2% agar tube and a 20 x 60 mm piece of filter paper for 20-22 hour before conditioning. During conditioning, one of the odorants was combined with sugar on the filter paper, and the test was repeated for the other odorant, in a different group of flies. To test for long-term memory, trained flies were transferred back to the agar tube for 24h until the test. Memory performance was tested by allowing flies for 2 mins to choose between the odors presented during conditioning. Performance index (PI) was calculated as the number of flies approaching the conditioned odor minus the number of the flies going to the opposite direction, divided by the total number of flies in the test. A single PI value is the average score from the test with the reverse conditioning odor combination. Sets for which total number of flies was below 20 were discarded.

Statistical analysis: Statistical analyses were carried out using Graph-Pad Prism. Confidence interval was 95%, setting significance at $p<0.05$. Chi-square tests were carried out when comparing categorical data. Numerical data were tested first for their type of distributions. If data were distributed normally, unpaired Student t-tests were used to compare means between two groups and One Way ANOVA or Welch ANOVA for larger groups, followed by post-doc Dunnett test for multiple comparisons to a fixed control. Two Way ANOVA was used when comparisons to two variables were made. If data were not normally distributed, non-parametric Mann-Whitney U-test for 2 two group comparisons and Kruskal Wallis ANOVA for larger groups, followed by post-hoc Dunn's multiple comparisons test to a fixed control. Statistical details including full genotypes, sample sizes, tests and p values are provided in Supplementary Table S2.

SUPPLEMENTARY TEXT

Supplementary Figure S2

The DNT-2 receptors *Toll-6* and *kek-6* are expressed in an associative circuit

To visualise where the DNT-2 receptors Toll-6 and Kek-6 are expressed in the adult brain, we used:

1. *Toll-6Gal4* and *kek-6Gal4* to drive the expression of *FlyBbow1.1*. Toll-6>FlyBow+ neurons included PAMs and PPL2 (Figure 1H), whilst Kek-6>FlyBow+ neurons included PAL, PPL1, PPM2 and PPM3 clusters (Figure 1I).

To further verify the above data, we also visualised cell nuclei with *Toll-6>HistoneYFP* and *kek-6>HistoneYFP* and tested co-distribution with anti-TH in cell bodies. This revealed that 30% PAMs and 1 PPL1 neuron express *Toll-6* and around 4 PAM and 5 PPL1 neurons express *kek-6* (Figure S2D,E,G). Furthermore, we found that *Toll-2, Toll-5, Toll-7, Toll-8* were all expressed in PAMs (Figure S2F,G). Similarly, all PPL1s express *Toll-5* and multiple *Tolls* are expressed in at least 1 PPL1 (Figure S2G).

2. *Toll6>FlyBow1.1* strongly labelled mushroom body (MB) lobes [1] (Figure 1H) and *kek-6>FlyBow1.1* did too (Figure 1I). To discern non-Kenyon cell projections of Toll-6+ or Kek-6+ neurons onto MB lobes, we combined *Toll6>FlyBow1.1* or *kek-6>FlyBow1.1* with *MB247-Gal80*, which inhibits Gal4 in Kenyon cells. This revealed Toll-6+ projections from PAM-α1, PAM-β2β'2 and PPL1-γped dopaminergic neurons (Figure S2A). In addition, we combined *Toll-6>CD8-RFP* with *R14C08-LexA>CD8-GFP* and co-localising signal showed that Mushroom Body Output Neuron (MBON)-M4M6 neurons are Toll-6+ as well (Figure S2C). Similarly, we identified Kek-6+ neuron projections from PPL1-γ2α'1 and/or MBON-γ2α'1 onto MB-γ2α'1, from PPL1-α2α'2 on MB α2α'2 and from PPL1-γped on MB-ped (Figure S2A,B).

3. We used MCFO to stochastically label *Toll-6* and *kek-6* expressing neurons. This revealed *Toll-6>MCFO+* $\alpha\beta$ core, $\alpha\beta$ surface and γ medial Kenyon Cells (Figure 1J); and *kek-6>MCFO+* $\alpha\beta$ and $\alpha'\beta'$ Kenyon cells, as well as PPL1 γ2α'1 and α2α'2 neurons (Figure 1K). Using MCFO, we identified Kek-6+ single-cell clones as DAL neurons (Figure 1M, identified most likely as ID: 5813047772 using NeuPrint), meaning that *kek-6* is expressed in DAL neurons.

4. Expression from a DAL neuron reporter (*DAL-LexA>CD8-GFP*) colocalised with Toll-6 (*Toll-6GAL4>10xCD8-RFP*)(Figure S2H) and Kek-6 (*kek-6-6GAL4>10xCD8-RFP)* reporters (Figure S2I), demonstrating that DAL neurons express both *Toll-6* and *kek-6.*

5. Analysis of published single-cell RNAseq data [74, 118] confirmed our findings that multiple *Tolls, keks* and their downstream signalling effectors, are expressed in PAM, PAL and PPL1 dopaminergic neurons, Kenyon cells, DAL neurons and across all mushroom body output neuron types (Figure S2G, Supplementary Table S1).

In summary, the DNT-2 receptors Toll-6 and Kek-6 are expressed in Kenyon cells, DAN, DAL and MBONs.

REFERENCES

1. Li G, Forero MG, Wentzell JS, Durmus I, Wolf R, Anthoney NC, et al. A Toll-receptor map underlies structural brain plasticity. Elife. 2020;9. Epub 2020/02/19. doi: 10.7554/eLife.52743. PubMed PMID: 32066523; PubMed Central PMCID: PMCPMC7077983.

2. Foldi I, Anthoney N, Harrison N, Gangloff M, Verstak B, Nallasivan MP, et al. Three-tier regulation of cell number plasticity by neurotrophins and Tolls in Drosophila. J Cell Biol. 2017;216(5):1421-38. Epub 2017/04/05. doi: 10.1083/jcb.201607098. PubMed PMID: 28373203; PubMed Central PMCID: PMCPMC5412559.

3. McIlroy G, Foldi I, Aurikko J, Wentzell JS, Lim MA, Fenton JC, et al. Toll-6 and Toll-7 function as neurotrophin receptors in the Drosophila melanogaster CNS. Nat Neurosci. 2013;16(9):1248-56. Epub 2013/07/31. doi: 10.1038/nn.3474. PubMed PMID: 23892553; PubMed Central PMCID: PMCPMC4634317.

4. Holtmaat A, Svoboda K. Experience-dependent structural synaptic plasticity in the mammalian brain. Nat Rev Neurosci. 2009;10(9):647-58. Epub 2009/08/21. doi: 10.1038/nrn2699. PubMed PMID: 19693029.

5. Deng W, Aimone JB, Gage FH. New neurons and new memories: how does adult hippocampal neurogenesis affect learning and memory? Nat Rev Neurosci. 2010;11(5):339-50. Epub 2010/04/01. doi: 10.1038/nrn2822. PubMed PMID: 20354534; PubMed Central PMCID: PMCPMC2886712.

6. Woollett K, Maguire EA. Acquiring "the Knowledge" of London's layout drives structural brain changes. Curr Biol. 2011;21(24):2109-14. Epub 2011/12/16. doi: 10.1016/j.cub.2011.11.018. PubMed PMID: 22169537; PubMed Central PMCID: PMCPMC3268356.

7. Li C, Liu SY, Pi W, Zhang PX. Cortical plasticity and nerve regeneration after peripheral nerve injury. Neural Regen Res. 2021;16(8):1518-23. Epub 2021/01/13. doi: 10.4103/1673-5374.303008. PubMed PMID: 33433465; PubMed Central PMCID: PMCPMC8323687.

8. Bharmauria V, Ouelhazi A, Lussiez R, Molotchnikoff S. Adaptation-induced plasticity in the sensory cortex. J Neurophysiol. 2022;128(4):946-62. Epub 2022/09/22. doi: 10.1152/jn.00114.2022. PubMed PMID: 36130163.

9. Wohleb ES, Franklin T, Iwata M, Duman RS. Integrating neuroimmune systems in the neurobiology of depression. Nat Rev Neurosci. 2016;17(8):497-511. Epub 2016/06/10. doi: 10.1038/nrn.2016.69. PubMed PMID: 27277867.

10. Krishnan V, Nestler EJ. The molecular neurobiology of depression. Nature. 2008;455(7215):894-902. Epub 2008/10/17. doi: 10.1038/nature07455. PubMed PMID: 18923511; PubMed Central PMCID: PMCPMC2721780.

11. Wang CS, Kavalali ET, Monteggia LM. BDNF signaling in context: From synaptic regulation to psychiatric disorders. Cell. 2022;185(1):62-76. Epub 2021/12/29. doi: 10.1016/j.cell.2021.12.003. PubMed PMID: 34963057; PubMed Central PMCID: PMCPMC8741740.

12. Casarotto PC, Girych M, Fred SM, Kovaleva V, Moliner R, Enkavi G, et al. Antidepressant drugs act by directly binding to TRKB neurotrophin receptors. Cell. 2021;184(5):1299-313 e19. Epub 2021/02/20. doi: 10.1016/j.cell.2021.01.034. PubMed PMID: 33606976; PubMed Central PMCID: PMCPMC7938888.

13. Barth M, Heisenberg M. Vision affects mushroom bodies and central complex in Drosophila melanogaster. Learn Mem. 1997;4(2):219-29. Epub 1997/07/01. doi: 10.1101/lm.4.2.219. PubMed PMID: 10456065.

14. Barth M, Hirsch HV, Meinertzhagen IA, Heisenberg M. Experience-dependent developmental plasticity in the optic lobe of Drosophila melanogaster. J Neurosci. 1997;17(4):1493-504. Epub 1997/02/15. PubMed PMID: 9006990; PubMed Central PMCID: PMCPMC6793721.

15. Heisenberg M, Heusipp M, Wanke C. Structural plasticity in the Drosophila brain. J Neurosci. 1995;15(3 Pt 1):1951-60. Epub 1995/03/01. PubMed PMID: 7891144; PubMed Central PMCID: PMCPMC6578107.

16. Baltruschat L, Prisco L, Ranft P, Lauritzen JS, Fiala A, Bock DD, et al. Circuit reorganization in the Drosophila mushroom body calyx accompanies memory consolidation. Cell Rep. 2021;34(11):108871. Epub 2021/03/18. doi: 10.1016/j.celrep.2021.108871. PubMed PMID: 33730583.

17. Kremer MC, Christiansen F, Leiss F, Paehler M, Knapek S, Andlauer TF, et al. Structural long-term changes at mushroom body input synapses. Curr Biol. 2010;20(21):1938-44. Epub 2010/10/19. doi: 10.1016/j.cub.2010.09.060. PubMed PMID: 20951043.

18. Sugie A, Hakeda-Suzuki S, Suzuki E, Silies M, Shimozono M, Mohl C, et al. Molecular Remodeling of the Presynaptic Active Zone of Drosophila Photoreceptors via Activity-Dependent Feedback. Neuron. 2015;86(3):711-25. Epub 2015/04/22. doi: 10.1016/j.neuron.2015.03.046. PubMed PMID: 25892303.

19. Linneweber GA, Andriatsilavo M, Dutta SB, Bengochea M, Hellbruegge L, Liu G, et al. A neurodevelopmental origin of behavioral individuality in the Drosophila visual system. Science. 2020;367(6482):1112-9. Epub 2020/03/07. doi: 10.1126/science.aaw7182. PubMed PMID: 32139539.

20. Sugie A, Marchetti G, Tavosanis G. Structural aspects of plasticity in the nervous system of Drosophila. Neural Dev. 2018;13(1):14. Epub 2018/07/02. doi: 10.1186/s13064-018-0111-z. PubMed PMID: 29960596; PubMed Central PMCID: PMCPMC6026517.

21. Sachse S, Rueckert E, Keller A, Okada R, Tanaka NK, Ito K, et al. Activity-dependent plasticity in an olfactory circuit. Neuron. 2007;56(5):838-50. Epub 2007/12/07. doi: 10.1016/j.neuron.2007.10.035. PubMed PMID: 18054860.

22. Technau GM. Fiber number in the mushroom bodies of adult Drosophila melanogaster depends on age, sex and experience. J Neurogenet. 1984;1(2):113-26. Epub 1984/04/01. doi: 10.3109/01677068409107077. PubMed PMID: 6085635.

23. Devaud JM, Acebes A, Ferrus A. Odor exposure causes central adaptation and morphological changes in selected olfactory glomeruli in Drosophila. J Neurosci. 2001;21(16):6274-82. Epub 2001/08/07. PubMed PMID: 11487650; PubMed Central PMCID: PMCPMC6763130.

24. Gorska-Andrzejak J, Keller A, Raabe T, Kilianek L, Pyza E. Structural daily rhythms in GFP-labelled neurons in the visual system of Drosophila melanogaster. Photochem Photobiol Sci. 2005;4(9):721-6. Epub 2005/08/27. doi: 10.1039/b417023g. PubMed PMID: 16121283.

25. Bushey D, Tononi G, Cirelli C. Sleep and synaptic homeostasis: structural evidence in Drosophila. Science. 2011;332(6037):1576-81. Epub 2011/06/28. doi: 10.1126/science.1202839. PubMed PMID: 21700878; PubMed Central PMCID: PMCPMC3128387.

26. Vaughen JP, Theisen E, Rivas-Serna IM, Berger AB, Kalakuntla P, Anreiter I, et al. Glial control of sphingolipid levels sculpts diurnal remodeling in a circadian circuit. Neuron. 2022;110(19):3186-205 e7. Epub 2022/08/13. doi: 10.1016/j.neuron.2022.07.016. PubMed PMID: 35961319.

27. Fernandez MP, Berni J, Ceriani MF. Circadian remodeling of neuronal circuits involved in rhythmic behavior. PLoS Biol. 2008;6(3):e69. Epub 2008/03/28. doi: 10.1371/journal.pbio.0060069. PubMed PMID: 18366255; PubMed Central PMCID: PMCPMC2270325.

28. Duhart JM, Herrero A, de la Cruz G, Ispizua JI, Pirez N, Ceriani MF. Circadian Structural Plasticity Drives Remodeling of E Cell Output. Curr Biol. 2020;30(24):5040-8 e5. Epub 2020/10/17. doi: 10.1016/j.cub.2020.09.057. PubMed PMID: 33065014.

29. Bolus H, Crocker K, Boekhoff-Falk G, Chtarbanova S. Modeling Neurodegenerative Disorders in Drosophila melanogaster. Int J Mol Sci. 2020;21(9). Epub 2020/05/03. doi: 10.3390/ijms21093055. PubMed PMID: 32357532; PubMed Central PMCID: PMCPMC7246467.

30. Riemensperger T, Isabel G, Coulom H, Neuser K, Seugnet L, Kume K, et al. Behavioral consequences of dopamine deficiency in the Drosophila central nervous system. Proc Natl Acad Sci U S A. 2011;108(2):834-9. doi: 10.1073/pnas.1010930108. PubMed PMID: 21187381; PubMed Central PMCID: PMCPMC3021077.

31. Waddell S. Reinforcement signalling in Drosophila; dopamine does it all after all. Curr Opin Neurobiol. 2013;23(3):324-9. Epub 2013/02/09. doi: 10.1016/j.conb.2013.01.005. PubMed PMID: 23391527; PubMed Central PMCID: PMCPMC3887340.

32. Waddell S. Dopamine reveals neural circuit mechanisms of fly memory. Trends in neurosciences. 2010;33(10):457-64. Epub 2010/08/13. doi: 10.1016/j.tins.2010.07.001. PubMed PMID: 20701984; PubMed Central PMCID: PMCPMC2947577.

33. Yamagata N, Ichinose T, Aso Y, Placais PY, Friedrich AB, Sima RJ, et al. Distinct dopamine neurons mediate reward signals for short- and long-term memories. Proc Natl Acad Sci U S A. 2015;112(2):578-83. Epub 2014/12/31. doi: 10.1073/pnas.1421930112. PubMed PMID: 25548178; PubMed Central PMCID: PMCPMC4299218.

34. Adel M, Griffith LC. The Role of Dopamine in Associative Learning in Drosophila: An Updated Unified Model. Neurosci Bull. 2021;37(6):831-52. Epub 2021/03/30. doi: 10.1007/s12264-021-00665-0. PubMed PMID: 33779893; PubMed Central PMCID: PMCPMC8192648.

35. Aso Y, Hattori D, Yu Y, Johnston RM, Iyer NA, Ngo TT, et al. The neuronal architecture of the mushroom body provides a logic for associative learning. Elife. 2014;3:e04577. Epub 2014/12/24. doi: 10.7554/eLife.04577. PubMed PMID: 25535793; PubMed Central PMCID: PMCPMC4273437.

36. Chen CC, Wu JK, Lin HW, Pai TP, Fu TF, Wu CL, et al. Visualizing long-term memory formation in two neurons of the Drosophila brain. Science. 2012;335(6069):678-85. Epub 2012/02/11. doi: 10.1126/science.1212735. PubMed PMID: 22323813.

37. Krashes MJ, Waddell S. Rapid consolidation to a radish and protein synthesis-dependent long-term memory after single-session appetitive olfactory conditioning in Drosophila. J Neurosci. 2008;28(12):3103-13. Epub 2008/03/21. doi: 10.1523/JNEUROSCI.5333-07.2008. PubMed PMID: 18354013; PubMed Central PMCID: PMCPMC2516741.

38. Placais PY, Trannoy S, Isabel G, Aso Y, Siwanowicz I, Belliart-Guerin G, et al. Slow oscillations in two pairs of dopaminergic neurons gate long-term memory formation in Drosophila. Nat Neurosci. 2012;15(4):592-9. Epub 2012/03/01. doi: 10.1038/nn.3055. PubMed PMID: 22366756.

39. Guven-Ozkan T, Davis RL. Functional neuroanatomy of Drosophila olfactory memory formation. Learn Mem. 2014;21(10):519-26. Epub 2014/09/17. doi: 10.1101/lm.034363.114. PubMed PMID: 25225297; PubMed Central PMCID: PMCPMC4175493.

40. Shields A, Amcheslavsky A, Brown E, Lee TV, Nie Y, Tanji T, et al. Toll-9 interacts with Toll-1 to mediate a feedback loop during apoptosis-induced proliferation in Drosophila. Cell Rep. 2022;39(7):110817. Epub 2022/05/19. doi: 10.1016/j.celrep.2022.110817. PubMed PMID: 35584678; PubMed Central PMCID: PMCPMC9211775.

41. Meyer SN, Amoyel M, Bergantinos C, de la Cova C, Schertel C, Basler K, et al. An ancient defense system eliminates unfit cells from developing tissues during cell competition. Science. 2014;346(6214):1258236. doi: 10.1126/science.1258236. PubMed PMID: 25477468; PubMed Central PMCID: PMCPMC5095928.

42. Pare AC, Vichas A, Fincher CT, Mirman Z, Farrell DL, Mainieri A, et al. A positional Toll receptor code directs convergent extension in Drosophila. Nature. 2014;515(7528):523-7. Epub 2014/11/05. doi: 10.1038/nature13953. PubMed PMID: 25363762; PubMed Central PMCID: PMCPMC4943584.

43. Tamada M, Shi J, Bourdot KS, Supriyatno S, Palmquist KH, Gutierrez-Ruiz OL, et al. Toll receptors remodel epithelia by directing planar-polarized Src and PI3K activity. Dev Cell. 2021;56(11):1589-602 e9. Epub 2021/05/02. doi: 10.1016/j.devcel.2021.04.012. PubMed PMID: 33932332; PubMed Central PMCID: PMCPMC8570296.

44. Ward A, Hong W, Favaloro V, Luo L. Toll receptors instruct axon and dendrite targeting and participate in synaptic partner matching in a Drosophila olfactory circuit. Neuron. 2015;85(5):1013-28. Epub 2015/03/06. doi: 10.1016/j.neuron.2015.02.003. PubMed PMID: 25741726; PubMed Central PMCID: PMCPMC4351475.

45. McLaughlin CN, Nechipurenko IV, Liu N, Broihier HT. A Toll receptor-FoxO pathway represses Pavarotti/MKLP1 to promote microtubule dynamics in motoneurons. J Cell Biol. 2016;214(4):459-74. Epub 2016/08/10. doi: 10.1083/jcb.201601014. PubMed PMID: 27502486; PubMed Central PMCID: PMCPMC4987293.

46. Weber AN, Tauszig-Delamasure S, Hoffmann JA, Lelievre E, Gascan H, Ray KP, et al. Binding of the Drosophila cytokine Spatzle to Toll is direct and establishes signaling. Nat Immunol. 2003;4(8):794-800. doi: 10.1038/ni955. PubMed PMID: 12872120.

47. Hoffmann A, Funkner A, Neumann P, Juhnke S, Walther M, Schierhorn A, et al. Biophysical characterization of refolded Drosophila Spatzle, a cystine knot protein, reveals distinct properties of three isoforms. J Biol Chem. 2008;283(47):32598-609. Epub 2008/09/16. doi: 10.1074/jbc.M801815200. PubMed PMID: 18790733.

48. Hoffmann A, Neumann P, Schierhorn A, Stubbs MT. Crystallization of Spatzle, a cystine-knot protein involved in embryonic development and innate immunity in Drosophila melanogaster. Acta Crystallogr Sect F Struct Biol Cryst Commun. 2008;64(Pt 8):707-10. Epub 2008/08/06. doi: 10.1107/S1744309108018812. PubMed PMID: 18678937; PubMed Central PMCID: PMCPMC2494967.

49. Lewis M, Arnot CJ, Beeston H, McCoy A, Ashcroft AE, Gay NJ, et al. Cytokine Spatzle binds to the Drosophila immunoreceptor Toll with a neurotrophin-like specificity and couples receptor activation. Proc Natl Acad Sci U S A. 2013;110(51):20461-6. Epub 2013/11/28. doi: 10.1073/pnas.1317002110. PubMed PMID: 24282309; PubMed Central PMCID: PMCPMC3870763.

50. DeLotto Y, DeLotto R. Proteolytic processing of the Drosophila Spatzle protein by easter generates a dimeric NGF-like molecule with ventralising activity. Mech Dev. 1998;72(1-2):141-8. Epub 1998/05/12. doi: 10.1016/s0925-4773(98)00024-0. PubMed PMID: 9533958.

51. Zhu B, Pennack JA, McQuilton P, Forero MG, Mizuguchi K, Sutcliffe B, et al. Drosophila neurotrophins reveal a common mechanism for nervous system formation. PLoS Biol. 2008;6(11):e284. doi: 10.1371/journal.pbio.0060284. PubMed PMID: 19018662; PubMed Central PMCID: PMCPMC2586362.

52. Park H, Poo MM. Neurotrophin regulation of neural circuit development and function. Nat Rev Neurosci. 2013;14(1):7-23. Epub 2012/12/21. doi: 10.1038/nrn3379. PubMed PMID: 23254191.

53. Yang T, Nie Z, Shu H, Kuang Y, Chen X, Cheng J, et al. The Role of BDNF on Neural Plasticity in Depression. Front Cell Neurosci. 2020;14:82. Epub 2020/05/01. doi: 10.3389/fncel.2020.00082. PubMed PMID: 32351365; PubMed Central PMCID: PMCPMC7174655.

54. Gay NJ, Gangloff M. Structure and function of Toll receptors and their ligands. Annu Rev Biochem. 2007;76:141-65. Epub 2007/03/17. doi: 10.1146/annurev.biochem.76.060305.151318. PubMed PMID: 17362201.

55. Leulier F, Lemaitre B. Toll-like receptors--taking an evolutionary approach. Nat Rev Genet. 2008;9(3):165-78. Epub 2008/01/30. doi: 10.1038/nrg2303. PubMed PMID: 18227810.

56. Ma Y, Li J, Chiu I, Wang Y, Sloane JA, Lu J, et al. Toll-like receptor 8 functions as a negative regulator of neurite outgrowth and inducer of neuronal apoptosis. J Cell Biol. 2006;175(2):209-15. Epub 2006/10/25. doi: 10.1083/jcb.200606016. PubMed PMID: 17060494; PubMed Central PMCID: PMCPMC2064562.

57. Okun E, Griffioen K, Barak B, Roberts NJ, Castro K, Pita MA, et al. Toll-like receptor 3 inhibits memory retention and constrains adult hippocampal neurogenesis. Proc Natl Acad Sci U S A. 2010;107(35):15625-30. Epub 2010/08/18. doi: 10.1073/pnas.1005807107. PubMed PMID: 20713712; PubMed Central PMCID: PMCPMC2932590.

58. Okun E, Griffioen KJ, Mattson MP. Toll-like receptor signaling in neural plasticity and disease. Trends in neurosciences. 2011;34(5):269-81. doi: 10.1016/j.tins.2011.02.005. PubMed PMID: 21419501; PubMed Central PMCID: PMC3095763.

59. Rolls A, Shechter R, London A, Ziv Y, Ronen A, Levy R, et al. Toll-like receptors modulate adult hippocampal neurogenesis. Nat Cell Biol. 2007;9(9):1081-8. Epub 2007/08/21. doi: 10.1038/ncb1629. PubMed PMID: 17704767.

60. Patel V, Patel AM, McArdle JJ. Synaptic abnormalities of mice lacking toll-like receptor (TLR)-9. Neuroscience. 2016;324:1-10. Epub 2016/03/10. doi: 10.1016/j.neuroscience.2016.03.001. PubMed PMID: 26955780.

61. Chen CY, Shih YC, Hung YF, Hsueh YP. Beyond defense: regulation of neuronal morphogenesis and brain functions via Toll-like receptors. J Biomed Sci. 2019;26(1):90. Epub 2019/11/07. doi: 10.1186/s12929-019-0584-z. PubMed PMID: 31684953; PubMed Central PMCID: PMCPMC6827257.

62. Mandai K, Guo T, St Hillaire C, Meabon JS, Kanning KC, Bothwell M, et al. LIG family receptor tyrosine kinase-associated proteins modulate growth factor signals during neural development. Neuron. 2009;63(5):614-27. Epub 2009/09/17. doi: 10.1016/j.neuron.2009.07.031. PubMed PMID: 19755105; PubMed Central PMCID: PMCPMC2758028.

63. Ulian-Benitez S, Bishop S, Foldi I, Wentzell J, Okenwa C, Forero MG, et al. Kek-6: A truncated-Trk-like receptor for Drosophila neurotrophin 2 regulates structural synaptic plasticity. PLoS Genet. 2017;13(8):e1006968. Epub 2017/08/29. doi: 10.1371/journal.pgen.1006968. PubMed PMID: 28846707; PubMed Central PMCID: PMCPMC5591008.

64. Minichiello L. TrkB signalling pathways in LTP and learning. Nat Rev Neurosci. 2009;10(12):850-60. Epub 2009/11/21. doi: 10.1038/nrn2738. PubMed PMID: 19927149.

65. Lu B, Pang PT, Woo NH. The yin and yang of neurotrophin action. Nat Rev Neurosci. 2005;6(8):603-14. Epub 2005/08/03. doi: 10.1038/nrn1726. PubMed PMID: 16062169.

66. Minichiello L, Calella AM, Medina DL, Bonhoeffer T, Klein R, Korte M. Mechanism of TrkB-mediated hippocampal long-term potentiation. Neuron. 2002;36(1):121-37. Epub 2002/10/09. doi: 10.1016/s0896-6273(02)00942-x. PubMed PMID: 12367511.

67. Tessarollo L, Yanpallewar S. TrkB Truncated Isoform Receptors as Transducers and Determinants of BDNF Functions. Front Neurosci. 2022;16:847572. Epub 2022/03/25. doi: 10.3389/fnins.2022.847572. PubMed PMID: 35321093; PubMed Central PMCID: PMCPMC8934854.

68. MacLaren CM, Evans TA, Alvarado D, Duffy JB. Comparative analysis of the Kekkon molecules, related members of the LIG superfamily. Dev Genes Evol. 2004;214(7):360-6. Epub 2004/06/05. doi: 10.1007/s00427-004-0414-4. PubMed PMID: 15179511.

69. Yasuda R, Hayashi Y, Hell JW. CaMKII: a central molecular organizer of synaptic plasticity, learning and memory. Nat Rev Neurosci. 2022;23(11):666-82. Epub 2022/09/03. doi: 10.1038/s41583-022-00624-2. PubMed PMID: 36056211.

70. Lu B, Nagappan G, Guan X, Nathan PJ, Wren P. BDNF-based synaptic repair as a disease-modifying strategy for neurodegenerative diseases. Nat Rev Neurosci. 2013;14(6):401-16. Epub 2013/05/16. doi: nrn3505 [pii]
10.1038/nrn3505. PubMed PMID: 23674053.

71. Costa M, Manton JD, Ostrovsky AD, Prohaska S, Jefferis GS. NBLAST: Rapid, Sensitive Comparison of Neuronal Structure and Construction of Neuron Family Databases. Neuron. 2016;91(2):293-311. Epub 2016/07/05. doi: 10.1016/j.neuron.2016.06.012. PubMed PMID: 27373836; PubMed Central PMCID: PMCPMC4961245.

72. Nern A, Pfeiffer BD, Rubin GM. Optimized tools for multicolor stochastic labeling reveal diverse stereotyped cell arrangements in the fly visual system. Proc Natl Acad Sci U S A. 2015;112(22):E2967-76. Epub 2015/05/13. doi: 10.1073/pnas.1506763112. PubMed PMID: 25964354; PubMed Central PMCID: PMCPMC4460454.

73. Mayseless O, Berns DS, Yu XM, Riemensperger T, Fiala A, Schuldiner O. Developmental Coordination during Olfactory Circuit Remodeling in Drosophila. Neuron. 2018;99(6):1204-15 e5. Epub 2018/08/28. doi: 10.1016/j.neuron.2018.07.050. PubMed PMID: 30146303.

74. Croset V, Treiber CD, Waddell S. Cellular diversity in the Drosophila midbrain revealed by single-cell transcriptomics. Elife. 2018;7. Epub 2018/04/20. doi: 10.7554/eLife.34550. PubMed PMID: 29671739; PubMed Central PMCID: PMCPMC5927767.

75. Cervantes-Sandoval I, Phan A, Chakraborty M, Davis RL. Reciprocal synapses between mushroom body and dopamine neurons form a positive feedback loop required for learning. Elife. 2017;6. Epub 2017/05/11. doi: 10.7554/eLife.23789. PubMed PMID: 28489528; PubMed Central PMCID: PMCPMC5425253.

76. Talay M, Richman EB, Snell NJ, Hartmann GG, Fisher JD, Sorkac A, et al. Transsynaptic Mapping of Second-Order Taste Neurons in Flies by trans-Tango. Neuron. 2017;96(4):783-95 e4. Epub 2017/11/07. doi: 10.1016/j.neuron.2017.10.011. PubMed PMID: 29107518; PubMed Central PMCID: PMCPMC5693608.

77. Cachero S, Gkantia M, Bates AS, Frechter S, Blackie L, McCarthy A, et al. BAcTrace a new tool for retrograde tracing of neuronal circuit. Nature Methods. 2020;17:1254-61. doi: 10.1101/2020.01.24.918656.

78. Arnot CJ, Gay NJ, Gangloff M. Molecular mechanism that induces activation of Spatzle, the ligand for the Drosophila Toll receptor. J Biol Chem. 2010;285(25):19502-9. Epub 2010/04/10. doi: 10.1074/jbc.M109.098186. PubMed PMID: 20378549; PubMed Central PMCID: PMCPMC2885229.

79. Neve KA, Seamans JK, Trantham-Davidson H. Dopamine receptor signaling. J Recept Signal Transduct Res. 2004;24(3):165-205. Epub 2004/11/04. doi: 10.1081/rrs-200029981. PubMed PMID: 15521361.

80. Hearn MG, Ren Y, McBride EW, Reveillaud I, Beinborn M, Kopin AS. A Drosophila dopamine 2-like receptor: Molecular characterization and identification of multiple alternatively spliced variants. Proc Natl Acad Sci U S A. 2002;99(22):14554-9. Epub 2002/10/23. doi: 10.1073/pnas.202498299. PubMed PMID: 12391323; PubMed Central PMCID: PMCPMC137921.

81. Shafer OT, Kim DJ, Dunbar-Yaffe R, Nikolaev VO, Lohse MJ, Taghert PH. Widespread receptivity to neuropeptide PDF throughout the neuronal circadian clock network of Drosophila revealed by real-time cyclic AMP imaging. Neuron. 2008;58(2):223-37. Epub 2008/04/29. doi: 10.1016/j.neuron.2008.02.018. PubMed PMID: 18439407; PubMed Central PMCID: PMCPMC2586874.

82. Liu C, Placais PY, Yamagata N, Pfeiffer BD, Aso Y, Friedrich AB, et al. A subset of dopamine neurons signals reward for odour memory in Drosophila. Nature. 2012;488(7412):512-6. Epub 2012/07/20. doi: 10.1038/nature11304. PubMed PMID: 22810589.

83. Feany MB, Bender WW. A Drosophila model of Parkinson's disease. Nature. 2000;404(6776):394-8. doi: 10.1038/35006074. PubMed PMID: 10746727.

84. Aso Y, Herb A, Ogueta M, Siwanowicz I, Templier T, Friedrich AB, et al. Three dopamine pathways induce aversive odor memories with different stability. PLoS Genet. 2012;8(7):e1002768. Epub 2012/07/19. doi: 10.1371/journal.pgen.1002768. PubMed PMID: 22807684; PubMed Central PMCID: PMCPMC3395599.

85. Aso Y, Siwanowicz I, Bracker L, Ito K, Kitamoto T, Tanimoto H. Specific dopaminergic neurons for the formation of labile aversive memory. Curr Biol. 2010;20(16):1445-51. Epub 2010/07/20. doi: 10.1016/j.cub.2010.06.048. PubMed PMID: 20637624; PubMed Central PMCID: PMCPMC2929706.

86. Scheunemann L, Placais PY, Dromard Y, Schwarzel M, Preat T. Dunce Phosphodiesterase Acts as a Checkpoint for Drosophila Long-Term Memory in a Pair of Serotonergic Neurons. Neuron. 2018;98(2):350-65 e5. Epub 2018/04/21. doi: 10.1016/j.neuron.2018.03.032. PubMed PMID: 29673482; PubMed Central PMCID: PMCPMC5919781.

87. Pech U, Revelo NH, Seitz KJ, Rizzoli SO, Fiala A. Optical dissection of experience-dependent pre- and postsynaptic plasticity in the Drosophila brain. Cell Rep. 2015;10(12):2083-95. Epub 2015/03/31. doi: 10.1016/j.celrep.2015.02.065. PubMed PMID: 25818295.

88. Riemensperger T, Issa AR, Pech U, Coulom H, Nguyen MV, Cassar M, et al. A single dopamine pathway underlies progressive locomotor deficits in a Drosophila model of Parkinson disease. Cell Rep. 2013;5(4):952-60. doi: 10.1016/j.celrep.2013.10.032. PubMed PMID: 24239353.

89. Sun J, Xu AQ, Giraud J, Poppinga H, Riemensperger T, Fiala A, et al. Neural Control of Startle-Induced Locomotion by the Mushroom Bodies and Associated Neurons in Drosophila. Front Syst Neurosci. 2018;12:6. Epub 2018/04/13. doi: 10.3389/fnsys.2018.00006. PubMed PMID: 29643770; PubMed Central PMCID: PMCPMC5882849.

90. Eyjolfsdottir E, Branson S, Burgos-Artizzu XP, Hoopfer ED, Schor J, Anderson DJ, et al., editors. Detecting Social Actions of Fruit Flies2014; Cham: Springer International Publishing.

91. Krashes MJ, Waddell S. Drosophila appetitive olfactory conditioning. Cold Spring Harb Protoc. 2011;2011(5):pdb prot5609. Epub 2011/05/04. doi: 10.1101/pdb.prot5609. PubMed PMID: 21536767.

92. Hyman C, Hofer M, Barde YA, Juhasz M, Yancopoulos GD, Squinto SP, et al. BDNF is a neurotrophic factor for dopaminergic neurons of the substantia nigra. Nature. 1991;350(6315):230-2. Epub 1991/03/21. doi: 10.1038/350230a0. PubMed PMID: 2005978.

93. Guillin O, Diaz J, Carroll P, Griffon N, Schwartz JC, Sokoloff P. BDNF controls dopamine D3 receptor expression and triggers behavioural sensitization. Nature. 2001;411(6833):86-9. Epub 2001/05/03. doi: 10.1038/35075076. PubMed PMID: 11333982.

94. Berton O, McClung CA, Dileone RJ, Krishnan V, Renthal W, Russo SJ, et al. Essential role of BDNF in the mesolimbic dopamine pathway in social defeat stress. Science. 2006;311(5762):864-8. Epub 2006/02/14. doi: 10.1126/science.1120972. PubMed PMID: 16469931.

95. Tauszig S, Jouanguy E, Hoffmann JA, Imler JL. Toll-related receptors and the control of antimicrobial peptide expression in Drosophila. Proc Natl Acad Sci U S A. 2000;97(19):10520-5. Epub 2000/09/06. doi: 10.1073/pnas.180130797. PubMed PMID: 10973475; PubMed Central PMCID: PMCPMC27057.

96. Hoffmann JA. The immune response of Drosophila. Nature. 2003;426(6962):33-8. Epub 2003/11/07. doi: 10.1038/nature02021. PubMed PMID: 14603309.

97. Hu X, Yagi Y, Tanji T, Zhou S, Ip YT. Multimerization and interaction of Toll and Spatzle in Drosophila. Proc Natl Acad Sci U S A. 2004;101(25):9369-74. Epub 2004/06/16. doi: 10.1073/pnas.0307062101. PubMed PMID: 15197269; PubMed Central PMCID: PMCPMC438983.

98. Martinowich K, Manji H, Lu B. New insights into BDNF function in depression and anxiety. Nat Neurosci. 2007;10(9):1089-93. Epub 2007/08/30. doi: 10.1038/nn1971. PubMed PMID: 17726474.

99. Fenner BM. Truncated TrkB: beyond a dominant negative receptor. Cytokine Growth Factor Rev. 2012;23(1-2):15-24. Epub 2012/02/22. doi: S1359-6101(12)00003-2 [pii] 10.1016/j.cytogfr.2012.01.002. PubMed PMID: 22341689.

100. Ohira K, Hayashi M. A new aspect of the TrkB signaling pathway in neural plasticity. Curr Neuropharmacol. 2009;7(4):276-85. Epub 2010/06/02. doi: 10.2174/157015909790031210. PubMed PMID: 20514207; PubMed Central PMCID: PMC2811861.

101. Ferrer I, Marin C, Rey MJ, Ribalta T, Goutan E, Blanco R, et al. BDNF and full-length and truncated TrkB expression in Alzheimer disease. Implications in therapeutic strategies. J Neuropathol Exp Neurol. 1999;58(7):729-39. PubMed PMID: 10411343.

102. Carim-Todd L, Bath KG, Fulgenzi G, Yanpallewar S, Jing D, Barrick CA, et al. Endogenous truncated TrkB.T1 receptor regulates neuronal complexity and TrkB kinase receptor function in vivo. J Neurosci. 2009;29(3):678-85. Epub 2009/01/23. doi: 10.1523/JNEUROSCI.5060-08.2009. PubMed PMID: 19158294; PubMed Central PMCID: PMCPMC2719435.

103. Yacoubian TA, Lo DC. Truncated and full-length TrkB receptors regulate distinct modes of dendritic growth. Nat Neurosci. 2000;3(4):342-9. Epub 2000/03/22. doi: 10.1038/73911. PubMed PMID: 10725923.

104. Ernst C, Deleva V, Deng X, Sequeira A, Pomarenski A, Klempan T, et al. Alternative splicing, methylation state, and expression profile of tropomyosin-related kinase B in the frontal cortex of suicide completers. Arch Gen Psychiatry. 2009;66(1):22-32. Epub 2009/01/07. doi: 10.1001/archpsyc.66.1.22. PubMed PMID: 19124685.

105. Blochl A, Sirrenberg C. Neurotrophins stimulate the release of dopamine from rat mesencephalic neurons via Trk and p75Lntr receptors. J Biol Chem. 1996;271(35):21100-7. Epub 1996/08/30. doi: 10.1074/jbc.271.35.21100. PubMed PMID: 8702878.

106. Sahu MP, Pazos-Boubeta Y, Pajanoja C, Rozov S, Panula P, Castren E. Neurotrophin receptor Ntrk2b function in the maintenance of dopamine and serotonin neurons in zebrafish. Sci Rep. 2019;9(1):2036. Epub 2019/02/16. doi: 10.1038/s41598-019-39347-3. PubMed PMID: 30765816; PubMed Central PMCID: PMCPMC6375947.

107. Stoilov P, Castren E, Stamm S. Analysis of the human TrkB gene genomic organization reveals novel TrkB isoforms, unusual gene length, and splicing mechanism. Biochem Biophys Res Commun. 2002;290(3):1054-65. Epub 2002/01/19. doi: 10.1006/bbrc.2001.6301. PubMed PMID: 11798182.

108. Fryer RH, Kaplan DR, Feinstein SC, Radeke MJ, Grayson DR, Kromer LF. Developmental and mature expression of full-length and truncated TrkB receptors in the rat forebrain. J Comp Neurol. 1996;374(1):21-40. Epub 1996/10/07. doi: 10.1002/(SICI)1096-9861(19961007)374:1<21::AID-CNE2>3.0.CO;2-P. PubMed PMID: 8891944.

109. Ohira K, Homma KJ, Hirai H, Nakamura S, Hayashi M. TrkB-T1 regulates the RhoA signaling and actin cytoskeleton in glioma cells. Biochem Biophys Res Commun. 2006;342(3):867-74. Epub 2006/02/28. doi: 10.1016/j.bbrc.2006.02.033. PubMed PMID: 16500620.

110. Adhikarla SV, Jha NK, Goswami VK, Sharma A, Bhardwaj A, Dey A, et al. TLR-Mediated Signal Transduction and Neurodegenerative Disorders. Brain Sci. 2021;11(11). Epub 2021/11/28. doi: 10.3390/brainsci11111373. PubMed PMID: 34827372; PubMed Central PMCID: PMCPMC8615980.

111. Figueroa-Hall LK, Paulus MP, Savitz J. Toll-Like Receptor Signaling in Depression. Psychoneuroendocrinology. 2020;121:104843. Epub 2020/09/11. doi: 10.1016/j.psyneuen.2020.104843. PubMed PMID: 32911436; PubMed Central PMCID: PMCPMC7883590.

112. Sharma A. Genome-wide expression analysis in epilepsy: a synthetic review. Curr Top Med Chem. 2012;12(9):1008-32. Epub 2012/02/23. doi: 10.2174/156802612800229189. PubMed PMID: 22352865.

113. Chan RF, Turecki G, Shabalin AA, Guintivano J, Zhao M, Xie LY, et al. Cell Type-Specific Methylome-wide Association Studies Implicate Neurotrophin and Innate Immune Signaling in Major Depressive Disorder. Biol Psychiatry. 2020;87(5):431-42. Epub 2020/01/01. doi: 10.1016/j.biopsych.2019.10.014. PubMed PMID: 31889537.

114. Garrett ME, Qin XJ, Mehta D, Dennis MF, Marx CE, Grant GA, et al. Gene Expression Analysis in Three Posttraumatic Stress Disorder Cohorts Implicates Inflammation and Innate Immunity Pathways and Uncovers Shared Genetic Risk With Major Depressive Disorder. Front Neurosci. 2021;15:678548. Epub 2021/08/17. doi: 10.3389/fnins.2021.678548. PubMed PMID: 34393704; PubMed Central PMCID: PMCPMC8358297.

115. Mehta D, Voisey J, Bruenig D, Harvey W, Morris CP, Lawford B, et al. Transcriptome analysis reveals novel genes and immune networks dysregulated in veterans with PTSD. Brain Behav Immun. 2018;74:133-42. Epub 2018/09/07. doi: 10.1016/j.bbi.2018.08.014. PubMed PMID: 30189241.

116. Yamazaki D, Hiroi M, Abe T, Shimizu K, Minami-Ohtsubo M, Maeyama Y, et al. Two Parallel Pathways Assign Opposing Odor Valences during Drosophila Memory Formation. Cell Rep. 2018;22(9):2346-58. Epub 2018/03/01. doi: 10.1016/j.celrep.2018.02.012. PubMed PMID: 29490271.

117. Ostrovsky A, Cachero S, Jefferis G. Clonal analysis of olfaction in Drosophila: image registration. Cold Spring Harb Protoc. 2013;2013(4):347-9. Epub 2013/04/03. doi: 10.1101/pdb.prot071738. PubMed PMID: 23547150.

118. Crocker A, Guan XJ, Murphy CT, Murthy M. Cell-Type-Specific Transcriptome Analysis in the Drosophila Mushroom Body Reveals Memory-Related Changes in Gene Expression. Cell Rep. 2016;15(7):1580-96. Epub 2016/05/11. doi: 10.1016/j.celrep.2016.04.046. PubMed PMID: 27160913; PubMed Central PMCID: PMCPMC5047377.

FIGURE LEGENDS

Figure 1 Neurons expressing *DNT-2* and its receptors *Toll-6* and *kek-6* in the adult brain

(A) DNT-2A expressing neurons (DNT-2>FlyBow1.1 in green; anti-Brp in magenta) have cell bodies in SOG and project to FLA/PRW and SMP. **(B,D)** Pre-synaptic (green) and post-synaptic (magenta) terminals of DNT-2A neurons seen with DNT-2>DenMark::RFP, Dsyd1::GFP, higher magnification in **(D),** different specimens from (B). **(D)** DNT-2A projections at SMP and PRW have both pre- and post-synaptic sites. **(C)** Single neuron DNT-2A>MCFO clones. **(E)** Left: DNT-2A neurons have the vesicular glutamate transporter vGlut (green). Right: Colocalization between Dop2RLex>AopCD8-GFP and DNT2Gal4>UASCD8-RFP in cell bodies of DNT-2A neurons (arrows). **(F)** Terminals of dopaminergic neurons (TH>mCD8GFP) abut and

overlap with those of DNT-2A neurons (DNT2>CD8-RFP, magenta), arrows. Dotted box indicates inset magnified on the right**. (G)** Illustration of neurons expressing DNT-2 (magenta) and its receptors, including KCs, DAN and DAL neurons. **(H)** *Toll-6>FlyBow1.1* is expressed in Kenyon cells, PPL2 and PAM DANs, as revealed by co-localization with anti-TH. **(I)** *kek-6>FlyBow1.1* co-localises with TH in MB vertical lobes, dopaminergic PALs, VUMs, PPL1, PPM2 and PPM3. **(J)** *Toll-6>MCFO* clones in MB neurons γ medial (γm), αβcore (αβc) and αβsurface (αβs). **(K)** *kek-6>MCFO* clones in MB Kenyon cells αβα'β'γ formed and MB γ2α'1 and α2α'2 and PPL1. **(L)** Relative projections of DNT-2 (magenta) and DAL (green) neurons, showing overlapping arborisations at SMP (right). **(M,O)** *kek-6>MCFO* clones in DAL neurons, MB neurons, fan shaped body and other neurons that arborise at PRW. SMP: superior medial protocerebrum, PRW: Prow, FLA: Flange, SOG: sub-aesophageal ganglion. Scale bars: (A-C, F-left,H,I,L-left,M,O) 50µm; (J,K,L-right) 30µm; (D,E,F-right) 25µm.

Figure 2 DNT-2 neurons are functionally connected to dopaminergic neurons

(A,C,E,F) TransTango revealed out-puts of DNT-2 neurons. **(A)** All neurons express TransTango and expression of the TransTango ligand in DNT-2 neurons identified DNT-2 out-puts with Tomato (anti-DsRed). **(C)** TransTango highlighted DNT-2 neurons, as all components are present in these cells. It revealed feedback connections between SPM and PRW/FLA (arrow). **(E,F)** Trans-Tango identified as DNT-2 outputs KC α'β' MB lobes (anterior brain, **E left**); Kenyon cell bodies (posterior, **E right**); DAL neurons **(F left,** arrows) and the dorsal layer of the fan shaped body **(F, right,** arrow). **(B,D)** BAcTrace tests connectivity to a candidate neuron input visualised with LexAop>sybGFP by driving the expression of a ligand from DNT-2GAL4 that will activate QUASTomato in the candidate input neuron [77]. **(D)** Top, control: BAcTrace controls for dopaminergic input to DNT-2A neurons at SMP: R58E02LexA>BAcTrace 806, no GAL4. PAM projections are revealed with GFP (green). Bottom, test: R58E02LexA, DNT-2GAL4>BAcTrace 806 revealed PAMs (magenta) are inputs of DNT-2A neurons at SMP. **(G)** qRT-PCR showing that TH mRNA levels increased with DNT-2 over-expression at 30°C *(tubGAL80^{ts}, DNT-2>DNT-2FL).* One way ANOVA, P=0.0085; post-doc Dunnett's multiple comparison test**. (H)** Optogenetic activation of DNT-2 neurons with UAS-

CsChrimson – with or without DNT-2 over-expression - excited PAM neurons, revealed with the Ca^{2+} reporter GCaMP6s *(DNT-2>CsChrimson, R58E02LexA>GCaMP6s)* in PAM projections at MB γ lobes. Ratiometric colouring, ROI shown in dashed lines. Pink line below traces indicates stimulation period. **(J)** FRET cAMP probe Epac1 revealed that *DNT-2>Dop2R-RNAi* knockdown decreased YFP/CFP ratio over time in DNT-2A neurons, meaning that cAMP levels increased. Two-way ANOVA, genotype factor p<0.0001, time factor p<0.0001; post-doc Dunnett's. **(I)** Summary: DNT-2 neurons and DANs are functionally connected and modulate each other. TH: tyrosine hydroxylase. Scale bars: (C-F) 50µm; (H) 20µm. P values over graphs in (I,J) refer to group analyses; stars indicate multiple comparisons tests. *p<0.05,**p<0.01, ***p<0.001. For sample sizes and further statistical details, see Supplementary Table S2.

Figure 3 DNT-2 and Toll-6 maintain PAM neuron survival in the developing and adult brain

(A) Illustration of PAM neuronal cell bodies and experimental temporal profile. DANs are shown in green, DNT-2A neurons in magenta and MB in grey. The left hemisphere shows the anterior brain with PAL and PAM DAN neurons (green) and DNT-2 neurons (magenta); the right shows the posterior brain, with the calyx and other DAN neurons (PPM1, PPM2, PPM3, PPL1, PPL2, green). In **(B-D)** fruit-flies were kept constantly at 25°C**. (B)** *DNT-2^{37}/DNT-2^{18}* mutants had fewer histone-YFP+ labelled PAM neurons. Un-paired Student t-test. **(C)** *Toll-6* RNAi knock-down in all DANs reduced Histone-YFP+ labelled PAM cell number. Un-paired Student t-test. **(D)** *DNT-2^{37}/DNT-2^{18}* mutants had fewer PAMs stained with anti-TH antibodies. Over-expressing *Toll-6^{CY}* in DANs rescued TH+ PAM neurons in *DNT-2^{37}/DNT-2^{18}* mutants, demonstrating that DNT-2 functions via Toll-6 to maintain PAM cell survival. Welch ANOVA p<0.0001, post-hoc Dunnett test. **(E-H)** Adult specific restricted over-expression or knock-down, using the GAL4 repressor *tubGAL80^{ts}*. **(E)** Adult specific *DNT-2* RNAi knockdown in DNT-2 neurons decreased Tomato-labelled PAM cell number. Un-paired Student t-test, p= 0.005. **(F)** Adult specific *Toll-6* RNAi knock-down in *Toll-6^{31}* heterozygous mutant flies in DANs, reduced Histone-YFP+ PAM cell number. Un-paired Student t-test, p= 0.0058. **(G)** PAMs were visualised with anti-TH. Left: *Toll-6>Toll-6-RNAi* knock-down decreased TH+ PAM cell number. Un-paired Student t-test, p= 0.0063, Right: *DNT-2>DNT-2-RNAi* knock-down decreased TH+ PAM cell number. Kruskal-

Wallis ANOVA, p=0.0001, post-hoc Dunn's test. **(H)** Adult-specific *DNT-2>DNT-2RNAi* knock-down increased the number of apoptotic cells in the brain labelled with anti-DCP-1. Dcp-1+ cells co-localise with anti-TH at least in PAM clusters. One Way ANOVA, p<0.0001, post-doc Bonferroni's multiple comparisons test. DANs>histone-YFP: all dopaminergic neurons expressing histone-YFP, genotype: THGal4 R58E02Gal4>UAS-histoneYFP. PAMsLexA>tomato: restricted to PAM DANs: R58E02LexA>LexAop-nlstdTomato. Controls: GAL4 drivers crossed to wild-type Canton-S. Scale bars: (B-G) 30µm; (H) 20µm. Graphs show box-plots around the median. P values over graphs in (D, G right, H) refer to group analyses; stars indicate multiple comparisons tests. *p<0.05, **p<0.01, ***p<0.001. For further genotypes, sample sizes and statistical details, see Supplementary Table S2.

Figure 4 DNT-2, Toll-6 and Kek-6 are required for arborisations and synapse formation in development and in the adult. (A-F) Fruit-flies were kept constantly at 25°C. **(A)** *Toll-6* RNAi knockdown (*MB301B>FB1.1, Toll-6-RNAi*) decreased PAM β2β'2 neuron dendrite complexity. Un-paired Student t-test p = 0.0018. **(B)** Over-expression of *DNT-2CK (MB301B>CD8-GFP, DNT-2CK)* increased PAM β2β'2 dendrite complexity. Un-paired Student t-test p = 0.0449. **(C)** Illustration showing the ROIs (dashed lines) used for the analyses, corresponding to dendrites of PAM and DAL neurons and axonal terminals of PPL1 neurons. **(D-E)** PPL1 axonal misrouting was visualised with *split-GAL4 MB320CGal4>FlyBow1.1.* Images show PPL1-γped neurons and some PPL1-α2α'2. **(D,D')** RNAi knock-down of *Toll-6, kek-6* or both in PPL1-γped neurons caused axonal terminal misrouting (arrows). **(D')** Higher magnification of **(D**, dotted squares**)**. Chi-square for group analysis: * p = 0.0224, and multiple comparisons Bonferroni correction control vs *Toll-6RNAi* **p<0.01; vs *kek-6RNAi* p<0.05; vs *Toll-6RNAi kek-6RNAi* **p<0.01, see Table S2**. (E)** PPL1 misrouting was also induced by over-expressed *DNT-2CK* or *DNT-2FL*. Chi-square for group analysis: *p<0.05, Bonferroni correction control vs *DNT-2CK* ns, vs *DNT-2FL* *p<0.05, see Table S2. **(F)** *DNT-2$^{37/18}$* mutants had reduced DAL dendrite complexity (terminal points, Student t test), size (dendrite length, Student t test), number of synapses (No. PSD, Student t test) and synapse density (PSD/total dendrite length, Student t test), and increased Homer-GFP+ PSD volume (Mann Whitney U test). **(G,H)** Adult specific RNAi knock-down or over-

expression in DAL neurons using *tubGAL80^{ts}.* DAL dendrites visualised with *G0431>Homer-GCAMP* and anti-GFP**. (G**) Over-expression of DNT-2CK or DNT-2FL decreased PSD volume. Kruskal Wallis ANOVA p<0.0001, post-hoc Dunn test. **(H)** DAL dendrites with Homer+ post-synaptic densities (PSD) (with overlaid rendering) showing that RNAi knock-down of *Toll-6* or *Toll-6 kek-6* decreased Homer+ PSD number and synapse density and increased PSD volume. Branch points: One way ANOVA p = 0.8606. PSD volume: One way ANOVA p<0.0001. No. Homer+ PSD: One way ANOVA p = 0.0002. Graphs show box-plots around the median or dots plots (PSD volume). P values over graphs in **(G,H)** refer to group analyses; asterisks indicate multiple comparisons tests to a fixed control in **(**grey). *p<0.05, **p<0.01, ***p<0.001, ****p<0.0001. Scale bars: (A,B,D) 30µm; (D', E,F,G,H) 20µm. For genotypes, sample sizes and statistical details, see Supplementary Table S2.

Figure 5 Neuronal-activity regulates DNT-2 and induced synapse formation. (A) Thermogenetic activation of DNT-2 neurons increased the number of DNT-2FLGFP+ vesicles or spots (*DNT-2>DNT-2-FL-GFP*, *TrpA1* with anti-GFP). Control 18°C: Unpaired Student t test, p = 0.7371. Activation 30°C 24h: Mann Whitney p = 0.0004**. (B)** Western blot from fly heads over-expressing DNT-2FL-GFP in DNT-2 neurons showing that neuronal activation with TrpA1 at 30°C increased DNT-2FL-GFP cleavage. Genotype: *DNT-2GAL4>UAS-TrpA1, UAS-DNT-2FL-GFP*. Controls are flies of the same genotype kept constantly at 18°C as well as flies treated also at 30°C but lacking TrpA1. **(C)** Thermoactivation of DNT-2 neurons altered DNT-2 arborisations, here showing an example with smaller dendrites and enlarged axonal arbours. **(D)** Thermogenetic activation of DNT-2 neurons increased the number of Homer+ PSDs in DNT-2 neurons, at SMP (*DNT-2>Homer-GCAMP3, TrpA1*, anti-GFP). Control 18°C: Unpaired Student t test, p = 0.0998. Test 30°C 24h: Unpaired Student t test p = 0.0204. See Table S2.

Figure 6 Neuronal activity induced synapse remodelling depended on DNT-2, Toll-6 and Kek-6. (A) Thermogenetic neuronal activation of DAL neurons with TrpA1 at 30°C after raising flies at 18°C, visualised in the SLP dendrite with Homer-GCaMP and anti-GFP antibodies (*G0431>homer-GCAMP, TrpA1)*. DAL

neuronal activity decreased dendrite complexity (terminal points, Mann Whitney U-test, p=0.0033) and size (dendrite length, Unpaired Student t test p<0.0001), it did not change PSD number (Unpaired Student t test p=0.2305) nor PSD volume (Mann Whitney U-test p=0.8653), but it increased synapse density (No. PSD/dendrite Length: Mann Whitney-U test p=0.028). Activity controls kept constantly at 18°C are provided in Supplementary Figure S5. **(B,D)** Compared to control *DNT-2^{37}/DNT-2^{18}* mutants kept at 18°C, neuronal thermoactivation of DAL neurons at 30°C in *DNT-2^{37}/DNT-2^{18}* mutants decreased terminal points further, did not alter dendrite size (total length), number of synapses (PSDs) nor synapse density (PSDs/total dendrite length), meaning that synaptic remodelling normally caused by neuronal activity did not occur in *DNT-2^{37}/DNT-2^{18}* mutants. PSD volume increased with activity. Terminal Points: Unpaired Student t test p =0.0216. Dendrite length: Unpaired Student t test p =0.0553. No. PSDs: Unpaired Student t test p =0.4064. Synapse density (No. PSDs/dendrite length): Mann Whitney U test p =0.2295. PSD volume: Mann Whitney U test p<0.0001. **(C,E)** Adult specific RNAi knock-down of *Toll-6* and *kek-6* reduced PSD number and synapse density and it increased PSD volume. Terminal Points: Unpaired Student t test p = 0.1189. Dendrite length: Unpaired Student t test p = 0.2755. No. PSDs: Unpaired Student t test p = 0.0043. Synapse density (No. PSDs/dendrite length): Unpaired Student t test p = 0.0104; PSD volume: Mann Whitney U test p<0.0001. Graphs show box-plots around the median, except for PSD volume data that are dot plots. p<0.05, **p<0.01, ***p<0.001, ****p<0.0001; ns: not significantly different from control. Scale bars: 30µm. For Genotypes, sample sizes and statistical details, see Supplementary Table S2.

Figure 7 DNT-2-induced circuit plasticity modified dopamine-dependent behaviour. (A) *DNT-2* mutants (left) and adult-specific RNAi knock-down of *DNT-2* in DNT-2 neurons (right), impaired climbing. Left Mann Whitney U: p=0.0357; Right: One Way ANOVA p<0.0001 (group analysis), post-hoc Dunnett. **(B)** Adult-specific *Toll-6* RNAi knock-down in Toll-6 *(Toll-6GAL4,* left) or PAM (*R58E02GAL4,* right) neurons impaired climbing. Left: Welch ANOVA p=0.0189, post-hoc Dunnett. Right: Welch ANOVA p=0.006, post-hoc Dunnett. **(C)** The climbing impairment of *DNT-2* mutants can be rescued with the over-expression of *Toll-6^{CY}* in dopaminergic neurons (*THGAL4 R58E02GAL4).* Welch ANOVA p=0.0058, post-hoc Dunnett. **(D)** Adult

specific *DNT-2FL* overexpression in DNT-2 neurons increased fruit-fly locomotion speed in an open arena. At 30°C: Kruskal-Wallis p<0.0001, post-hoc Dunn's test. **(E)** Thermogenetic activation of DNT-2 neurons *(DNT-2>TrpA1)* increased fruit-fly locomotion speed. Kruskal-Wallis p<0.0001, post-hoc Dunn's test**. (F)** *DNT-2^{37}/DNT-2^{18}* mutant flies had reduced appetitive learning and long-term memory. WT control: Canton-S/Oregon. Un-paired student t-test, p=0.0102. **(G)** Over-expression of *DNT-2-FL* in DNT-2 neurons increased long-term memory. Right 30°C: One Way ANOVA p<0.001, post-hoc Dunnett's test. **(H)** Thermogenetic activation of DNT-2 neurons increased long-term memory. Right 30°C: One Way ANOVA, post-hoc Dunnett test. Graphs show box-plots around the median, in (D-H) under also dot plots. P values over graphs refer to group analyses; asterisks indicate multiple comparisons tests. *p<0.05, **p<0.01, ***p<0.001, ****p<0.0001; ns: not significantly different from control. For Genotypes, sample sizes and statistical details, see Supplementary Table S2.

Figure 8 DNT-2 with a Toll and kinase-less Trk-like Kek receptors drives structural circuit plasticity modifying behaviour. Illustrative summary of findings. **(A)** A novel mechanism involving a neurotrophin functioning via Toll and kinase-less Trk-like Kek receptors regulates activity-dependent circuit plasticity. Neuronal activation – as a proxy for experience, shown instead in the diagram - caused the up-regulation and release of DNT-2, which up-regulated TH levels, conducive to increased dopamine production. DNT-2 and dopamine regulate each other, as dopamine induced negative feedback in DNT-2 neurons. Dopamine labelled neural circuits engaged and DNT-2 and its receptors induced structural circuit plasticity – i.e. synapse formation - modifying dopamine-dependent behaviour. **(B)** Drawing of the circuit elements analysed. DNT-2A neurons are connected to the dopaminergic and associative learning circuit involving Kenyon cells, PAM and PPL1 DANs and DAL neurons**. (D)** Altering the levels of DNT-2, Toll-6 and Kek-6 shifted the balance between structural brain plasticity and degeneration. Data showed that the neurotrophin ligand DNT-2 can promote dendrite growth and synapse formation, and that neuronal activity increased DNT-2 levels, which increased TH levels, and together increased locomotion and memory. By contrast, loss of function for DNT-2, Toll-6 and kek-6 led to PAM neuron apoptosis and loss, impaired dendrite and axonal arborisations and

synapse loss, and prevented activity-dependent synapse formation and remodelling, leading to impaired locomotion and memory, altogether features characteristic of neurodegeneration.

SUPPLEMENTAL INFORMATION

Supplementary Figure S1 Identification of neurotransmitter type for DNT- 2A neurons. (A) DNT-2-GAL4 expressing neurons neurons include anterior DNT-2A lateral neurons in GNG (left) and other neurons, including posterior neurons that arborise in PLP (right). **(B,C)** DNT-2 neurons are not dopaminergic, as there is no co-localisation between *DNT-2>histoneYFP* and anti-TH. Higher magnification of dotted boxes on the right. **(D)** DNT-2A neurons do not express the *Dop1R* dopamine receptor, as revealed by no colocalisation with *Dop1R2LexA>CD8::GFP, DNT-2Gal4>CD8::RFP*. **(E,F)** Neither anterior DNT-2A nor posterior DNT-2 neurons are octopaminergic, as there is no overlap between *TdcLexA>mCD8::GFP and DNT-2Gal4>CD8::RFP*. **(G)** DNT-2A neurons are not serotonergic, as there was no co-localization between *DNT-2>FlyBow1.1* and the serotoninergic neuron marker anti-5HT either. **(H)** There is no overlap either between *DNT-2Gal4>histoneYFP* and the cholinergic neuron marker anti-ChAT4b1. **(I,J)** Anterior DNT-2A neurons are not GABAergic, but lateral DNT-2 neurons are, as visualised with *DNT-2>CD8-RFp, GADLexA>CD8-GFP*. Scale bars: (A-C,E) 50µm; (D-J) 20 µm.

Supplementary Figure S2 Identification of *Toll-6* and *kek-6* expressing neurons. (A) *kek-6Gal4, MB247-Gal80>UASFlyBow1.1* revealed Kek-6+ projections on MB γ2α'1. **(B)** *R25D01LexA>CD8GFP, kek6-Gal4>CD8RFP* overlapped in MB γ2α'1. **(C)** *R14C08LexA>CD8GFP, Toll-6Gal4>CD8-RFP13* revealed co-localization in MBON-M4/M6 cell bodies. **(D,E)** Co-localisation of *Toll-6>Histone-YFP* and *kek-6>HistoneYFP* with TH in PAMs. **(F)** Co-localisation of *Toll-2>, Toll-5>, Toll-7>* and *Toll-8>Histone-YFP* with TH in PAM clusters reveals that PAMs express multiple *Tolls*, and most likely each PAM neuron expresses at least one *Toll.* **(G)** Number of PAM and PPL1 neurons expressing *Tolls* and *kek-6,* revealed from HistoneYFP and published RNAseq data (Scope) (see Table S1). **(H)** DAL neurons express *Toll-6,* as revealed by co-localization between *DAL-LexA (VT49239-LexA)>mCD8-GFP* and *Toll-6GAL4>mCD8-RFP*. **(I)** DAL neurons

express *kek-6*, as revealed by colocalization between *DAL-LexA (VT49239-LexA)>mCD8-GFP* and *kek6GAL4>mCD8RFP*. Scale bars: (D) 50µm; (A,C,F) 30µm.

Supplementary Figure S3 Connectivity controls and octopaminergic neuron input. (A) Left: *UAS-TransTango/+* control, showing background GFP expression in mushroom bodies and RFP signal in sub-aesophageal ganglion (SOG). **Right:** *DNT-2GAL4>UAS-TransTango*, revealing the GFP+ DNT-2 neurons and RFP+ signal in DNT-2 neurons. TransTango also reveals what appears to be feedback connections between DNT-2 neurons from SMP to PRW (arrow). **(B) Left:** BAcTrace controls*: Tdc2LexA>BAcTrace,* no GAL4. GFP signal reveals the expression of Tdc2 in candidate octopaminergic input neurons being tested. There is mild RFP background. **Right:** *Tdc2 LexA, DNT-2GAL4>BAcTrace*, revealing with GFP (green) the *Tdc2* expressing neurons and in magenta (co-localising green + magenta in white) Tdc2+ neurons identified as DNT-2 inputs at PRW. Scale bars: (A,B) 50µm.

Supplementary Figure S4 Over-expression of DNT-2 in the adult brain reduced PSD volume. (A) Regime used for the over-expression of DNT-2 in the adult brain. **(B,C)** DNT-2CK or DNT-2FL over-expression in DAL neurons *(tubGAL80ts, DAL-GAL4>Homer-GCaMP, DNT-2CK or FL)* did not alter dendrite complexity (terminal points), size (dendrite length), number of synapses (Homer-GFP+ PSDs) nor synapse density (PSD/dendrite length), but it decreased PSD volume. Terminal points: One Way ANOVA p=0.1161. Dendrite length: One Way ANOVA p=0.2592. Number of synapses (Homer-GFP+ PSDs): One Way ANOVA p=0.1195. Synapse density (PSD/total dendrite length): One Way ANOVA p=0.0494. PSD Volume: Kruskal-Wallis ANOVA p<0.0001**;** post-hoc Dunn test. Graphs show box-plots around the median, except for PSD volume that are dot plots. Values over graphs refer to group analyses; asterisks indicate multiple comparisons tests. *p<0.05, **p<0.01, ***p<0.001, ****p<0.0001; ns: not significantly different from control. For Genotypes, sample sizes and statistical details, see Supplementary Table S2.

Supplementary Figure S5 **Activity controls at 18°C for Figure 6A**. Controls for thermogenetic neuronal activation of DAL neurons, whereby control flies with and without TrpA1 were raised at 18°C and kept constantly at 18°C. DAL-SLP dendrites were visualised with Homer-GCaMP and anti-GFP antibodies (*G0431>homer-GCAMP* and *G0431>homer-GCAMP, TrpA1* at 18°C). No major structural changes in DAL-SLP dendrites were observed at 18°C. Terminal points: Man Whitney U test: p=0.0257. Dendrite length: Student t test p=0.1136. No of PSD: Student t test p=0.4427. Synapse density (PSD/dendrite length): Mann Whitney U test p=0.4202. PSD volume: Mann Whitney U test p=0.2141.

Supplementary Figure S6 **Altering *DNT-2* levels induced seizures.** Knock-down or over-expression of *DNT-2* in the adult, using *GAL80^{ts}*. Fruit-flies were reared at 18°C from egg laying to adult eclosion, when they were transferred to 30°C and kept there for 5 days prior to testing**.** To test for seizures, we used the bang-sensitivity test. *DNT2^{37}/DNT2^{18}* mutant flies and adult *DNT-2* knock-down flies (*tubGal80^{ts} DNT-2Gal4>DNT-2RNAi)* took longer to recover than controls. Over-expression of *DNT-2FL* in DNT-2 neurons (*tubGal80^{ts} DNT-2Gal4>DNT-2FL*) increased variability in recovery time.

Table S1 **Expression of *Tolls, keks* and Toll downstream adaptors in cells related to DNT-2A neurons.** Genes expressed in DNT-2 neurons, their potential and/or experimentally verified inputs and outputs, were identified with a combination of reporters (this work) and data from public single-cell RNAseq databases.

Table S2 **Statistical analysis.** Table providing all genotypes, sample sizes, statistical tests and p values.

FIGURE 1 Neurons expressing *DNT-2* and its receptors *Toll-6* and *kek-6* in the adult brain

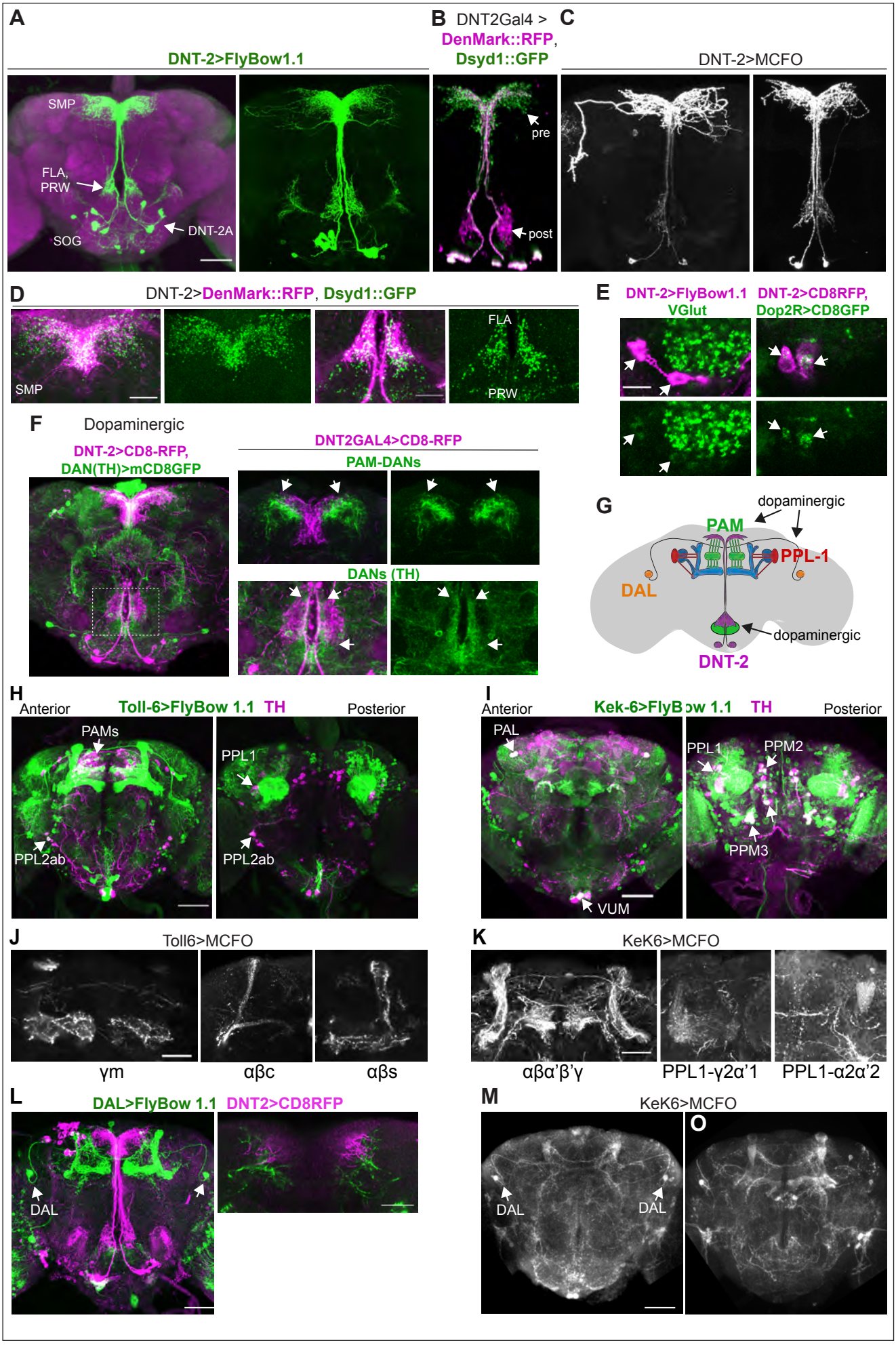

Figure 2 DNT-2 neurons are functionally connected to dopaminergic neurons

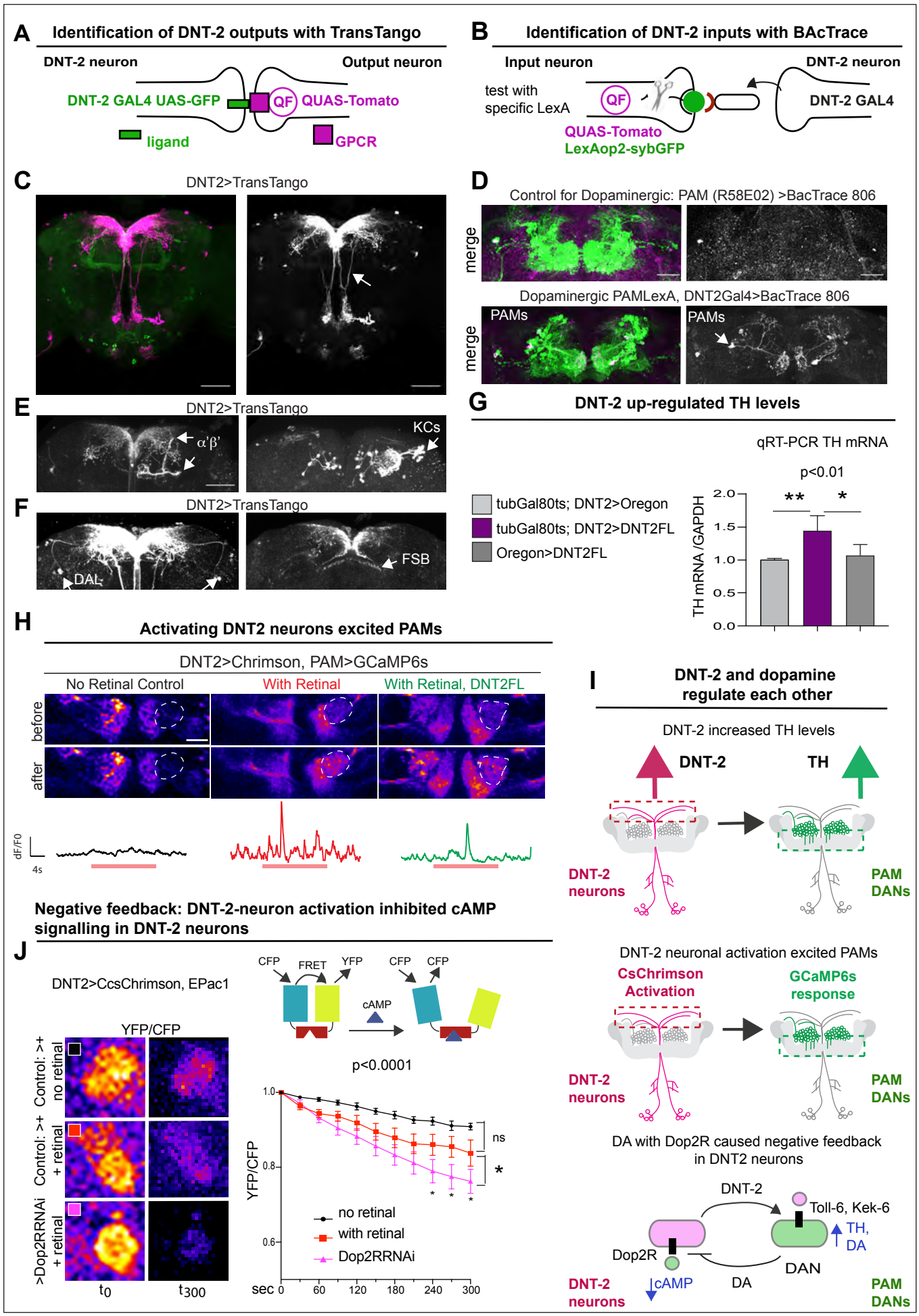

Figure 3 DNT-2 and Toll-6 maintain PAM neuron survival in the developing and adult brain

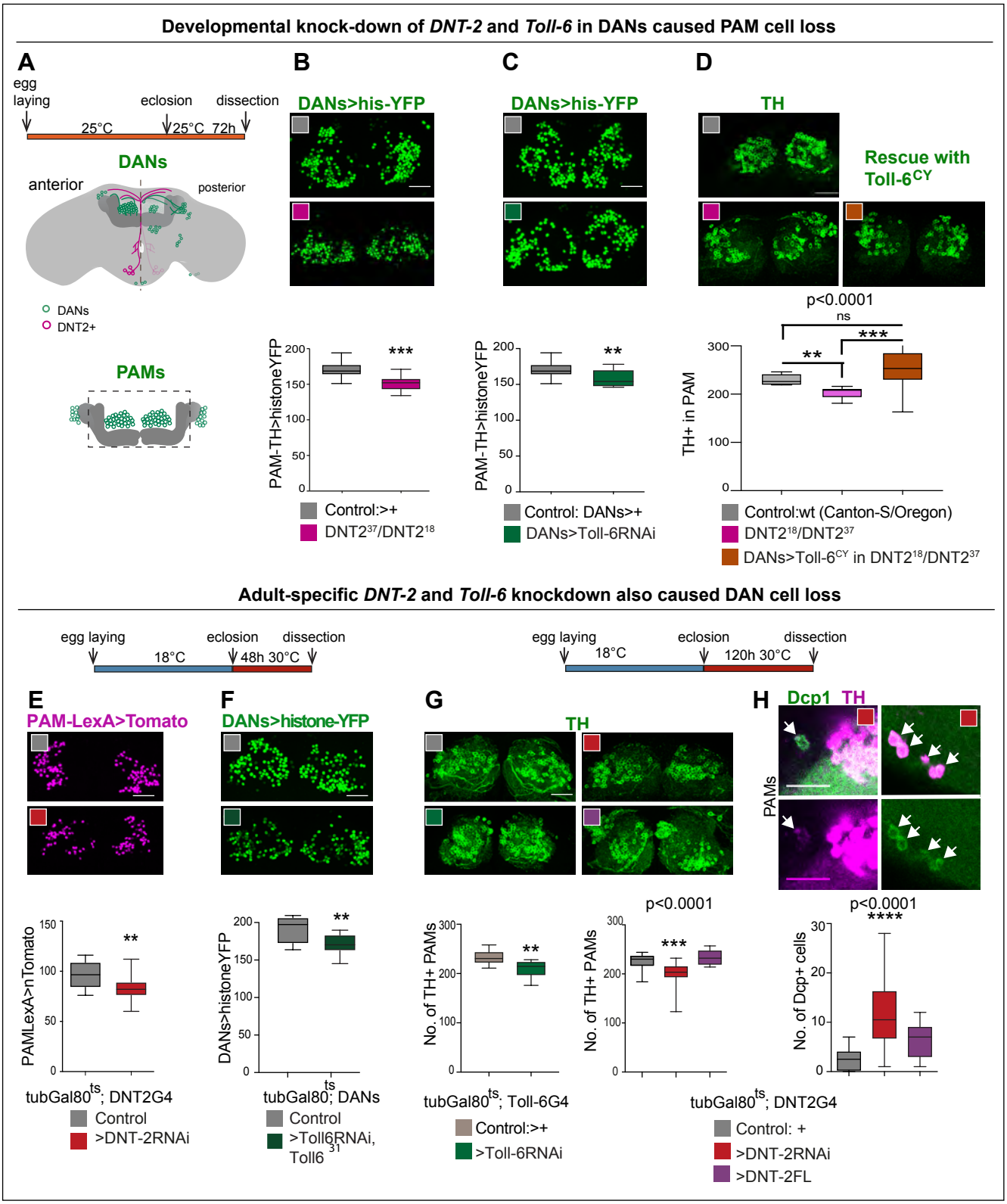

Figure 4 DNT-2, Toll-6 and Kek-6 are required for arborisations and synapse formation in development and in the adult.

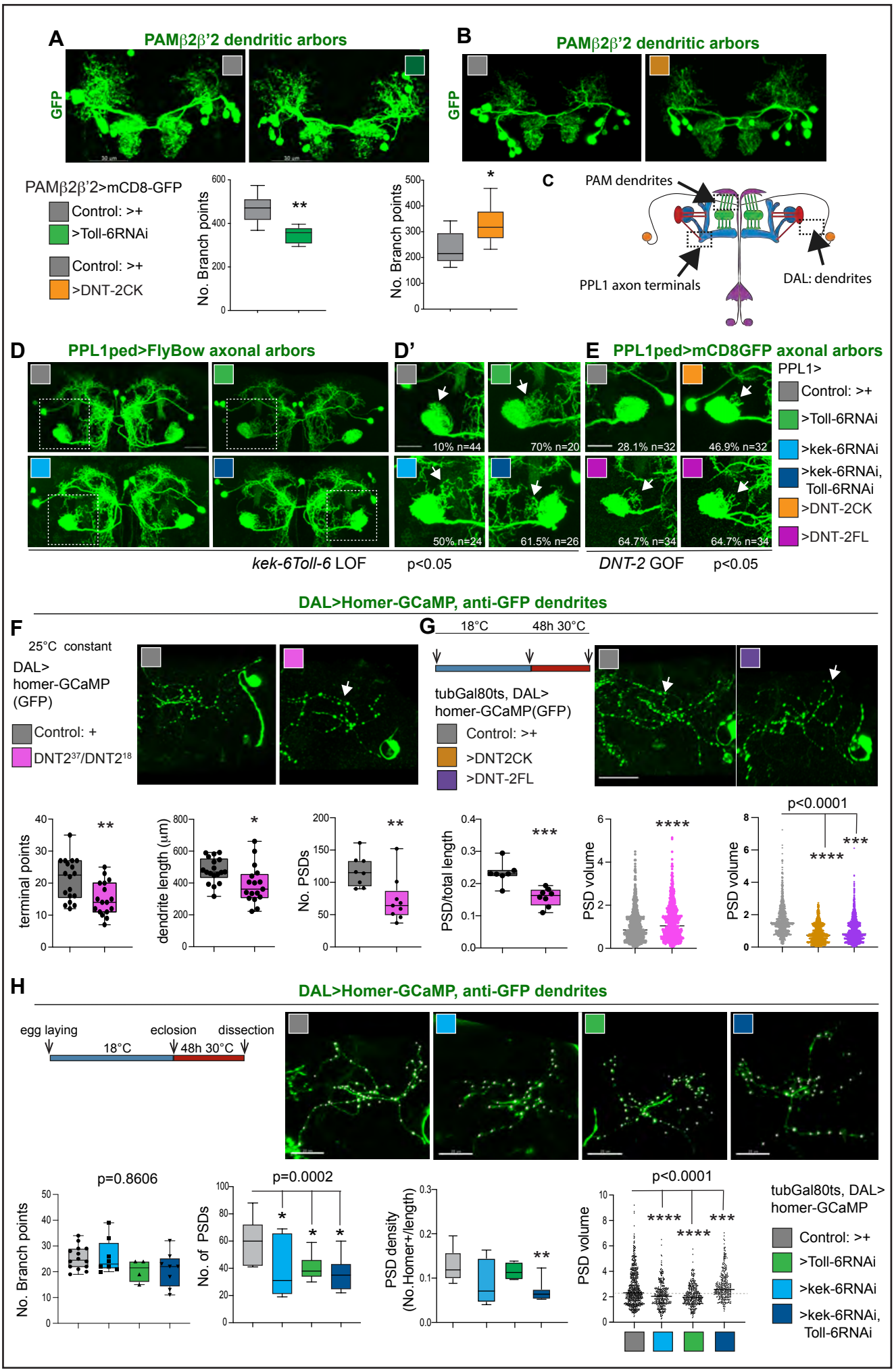

Figure 5 Neuronal activity regulates DNT-2 and induced synapse formation.

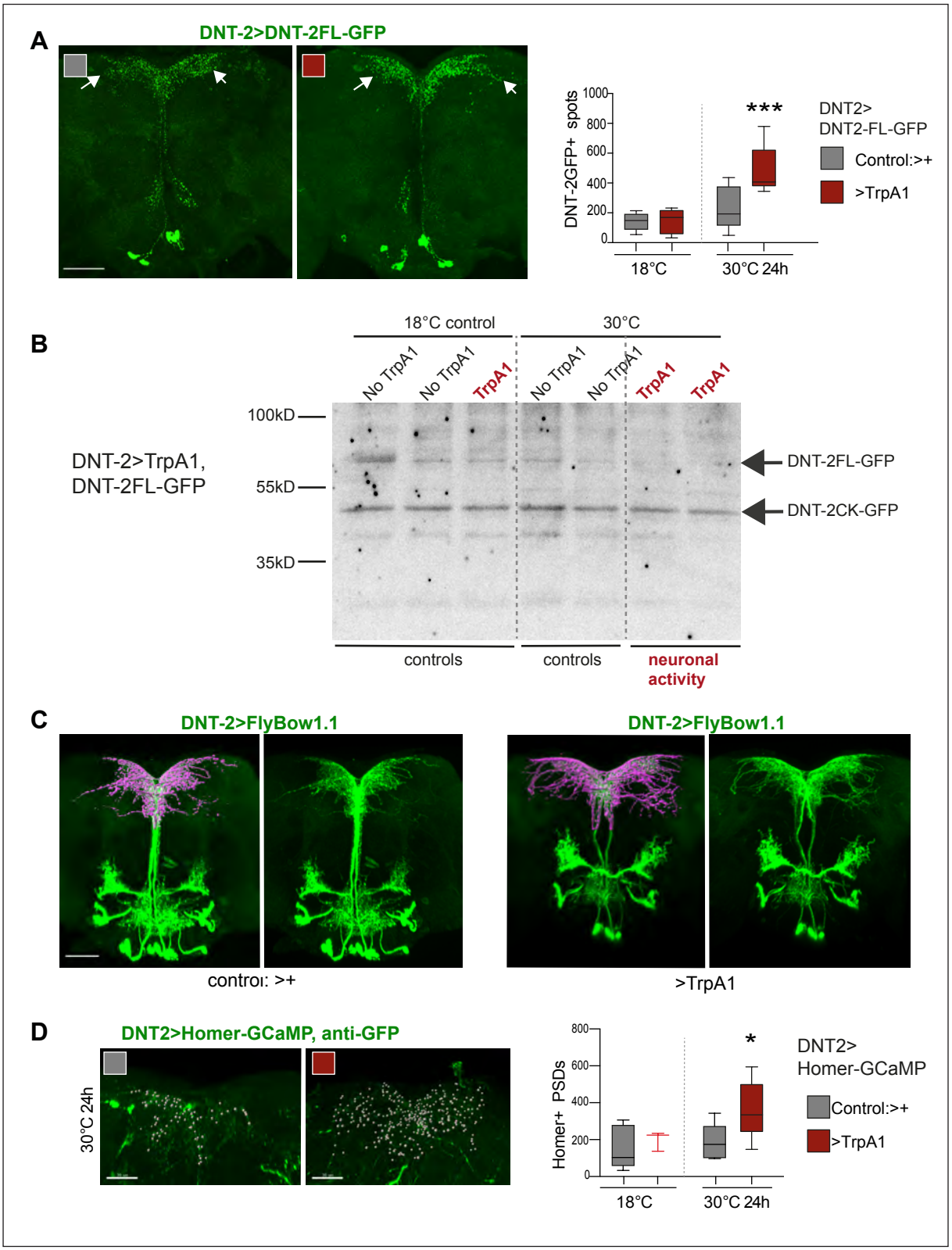

Figure 6 Neuronal activity induced synapse remodelling depended on DNT-2, Toll-6 and kek-6

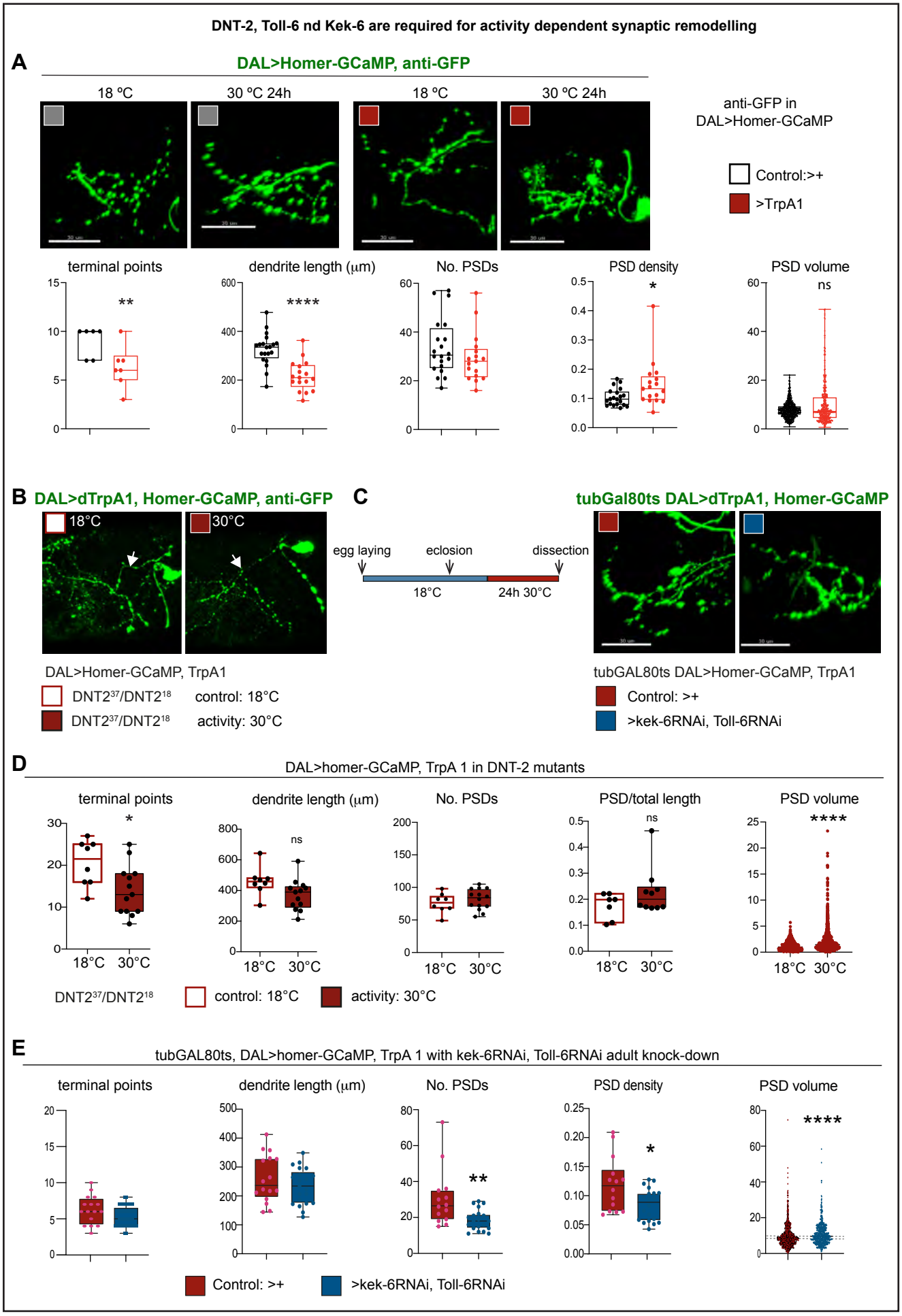

Figure 7 DNT-2-induced circuit plasticity modified dopamine-dependent behaviours.

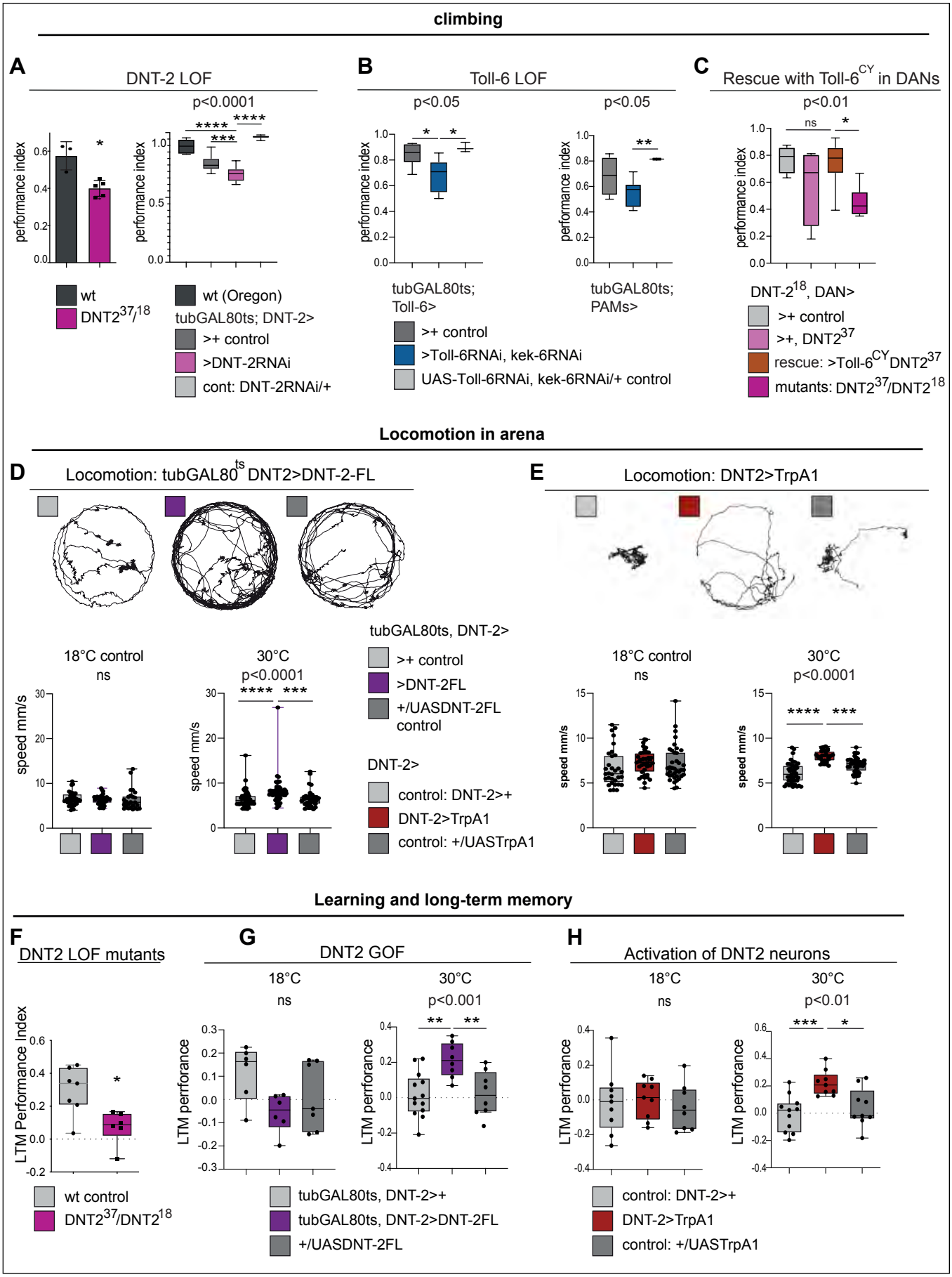
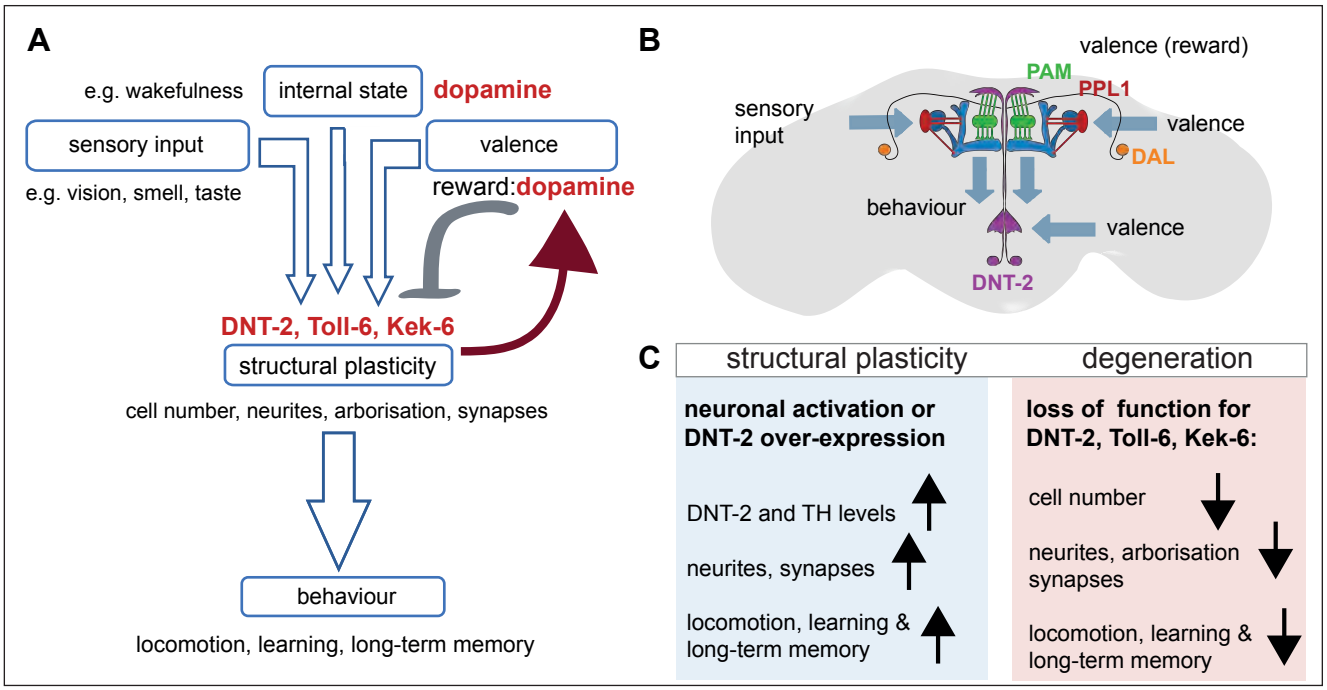
FIGURE 8
DNT-2 with a Toll and kinase-less Trk-like Kek receptors drives structural circuit plasticity modifying behaviour